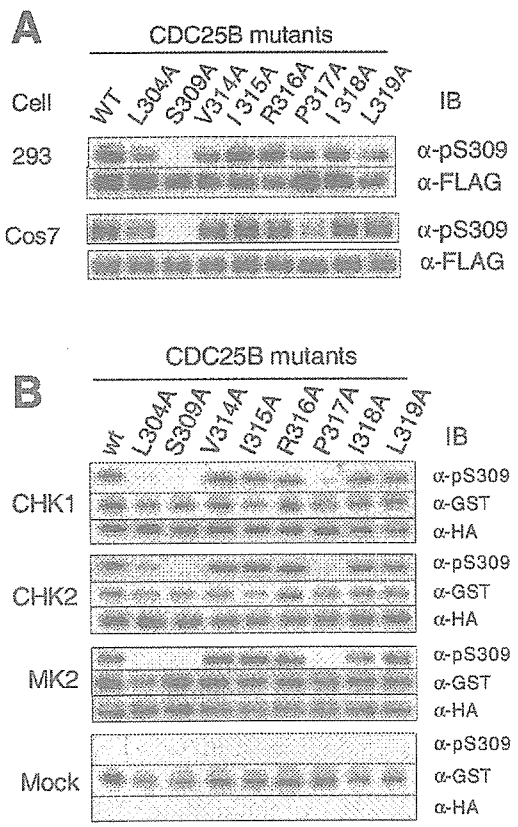

Fig. 4. **Phosphorylation of Ser309 *in vivo* and *in vitro* by representative kinases.** HEK293 cells (1.4×10^6 cells per 35-mm plate) or Cos-7 cells (2×10^5 cells per 35-mm plate) were transfected with plasmids carrying FLAG-tagged CDC25B mutants, and the expressed proteins were immunoprecipitated with monoclonal anti-FLAG beads. The precipitated proteins were immunoblotted with anti-FLAG or anti-phospho-Ser309 antibodies (A). His- and HA-tagged kinases were expressed in Cos-7 cells and recovered as described. The recovered kinases were incubated with GST-fused CDC25B peptides (wild-type or mutant), and phosphorylation at Ser309 was determined by immunoblotting (B).

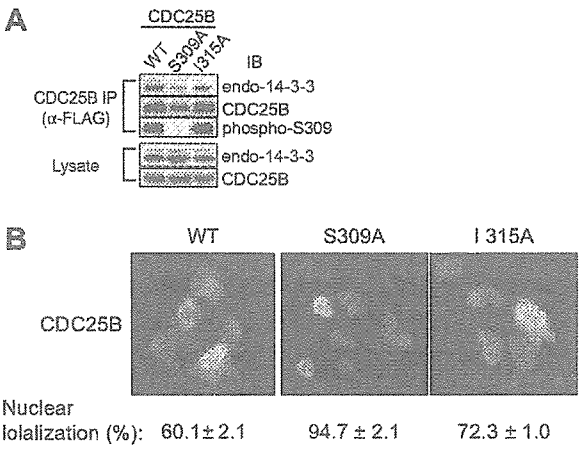

Fig. 5. **Binding of endogenous 14-3-3 to CDC25B mutants and subcellular localization.** HEK293 cells were transfected with plasmids carrying wild type CDC25B or Ala309 or Ala315 mutants, and the expressed proteins were recovered with anti-FLAG beads. The precipitates were immunoblotted with an anti-pan 14-3-3 antibody (upper panel), anti-FLAG antibody (second panel), or anti–phospho-Ser309 antibody (third panel). The expression of endogenous 14-3-3 and transfected CDC25B is indicated in the two bottom panels (A). HEK293 cells were transfected with CDC25B plasmids as in (A), and the subcellular localization of the expressed CDC25B proteins was determined as in Fig. 2D. The numbers represent the percentages of cells expressing the CDC25B protein found exclusively in the nucleus. Three independent experiments were performed for each value , and more than 200 CDC25B-expressing cells were counted in each experiment (B).

CHK1 (*18*), CHK2 (*19*) and MK2 (*26*) in Cos-7 cells and then recovered the kinases by immunoprecipitation. For the preparation of MK2, an upstream kinase, mitogen-activated protein kinase kinase kinase 6 (MKK6) and MK2 were co-transfected, and the expressed MK2 was immunoprecipitated. An *in vitro* phosphorylation assay indicated that the three kinases could phosphorylate GST-tagged CDC25B mutant peptides (Fig. 4B), the results being similar to those obtained *in vivo* (Fig. 4A). The kinases phosphorylated all of the mutant peptides with similar efficiency, with the exception of the Pro317Ala mutant, consistent with the results shown in Fig. 4A. These results demonstrate that Ser309 of CDC25B can be phosphorylated by several kinases.

Binding of Endogenous 14-3-3 to CDC25B Mutants and Their Subcellular Localization—We examined the binding of endogenous 14-3-3 to mutant CDC25B proteins. After transfection to HEK293 cells, CDC25B proteins were recovered, and the bound 14-3-3 protein was quantitated using a pan-14-3-3 antibody. Figure 5A shows that the efficiency of endogenous 14-3-3 binding to mutant CDC25B was similar to that in the co-expression experiments. Endogenous 14-3-3 bound to wild-type CDC25B most efficiently and to the 309Ala mutant least efficiently. A lesser amount of endogenous 14-3-3 was detected with the 315Ala mutant, which exactly matched the results in Fig. 3C and D. The phosphorylation of S309 in the I315A mutant could also be reproduced (compare Figs. 5A and 4A). We examined the subcellular localization of these mutant CDC25B proteins expressed in cells (Fig. 5B). The number of cells with CDC25B specifically localized in the nucleus was higher for mutant CDC25B than for the wild-type protein. About 72% of the cells exhibited specific nuclear localization of CDC25B 315Ala mutants, which was higher than the frequency of nuclear localization of wild-type CDC25B (~60%). Collectively, amino acid sequences surrounding the 14-3-3 binding core consensus site have a strong influence on 14-3-3 binding but subcellular localization of CDC25B can not be simply explained by 14-3-3 binding.

Finally, the results of this study are summarized in Table 3.

DISCUSSION

Seven isoforms of 14-3-3 have been identified in mammalian cells. We previously reported that three isoforms, 14-3-3β, ε, and σ, are able to bind to CDC25B, and that the

Table 3. **Summary of 14-3-3β binding and Ser309 phosphorylation of each CDC25B mutant.**

Name	Sequence	14-3-3β Binding (%)	Ser309 phosphorylation	
			in vivo	*in vitro*
WT	^{304}LFRSPSMPCSVIRPILKR^{321}	100	+	+
GS	LFRSPSMPCSVIRPILGSKR	17	+	NT
L304A	A----------KR	70	+	±
R306A	--A----------KR	23	NT	NT
S309A	-----A----------KR	18	–	–
M310A	------A---------KR	60	NT	NT
P311A	-------A--------KR	25	NT	NT
C312A	--------A-------KR	103	NT	NT
S313A	---------A------KR	63	NT	NT
V314A	----------A-----KR	21	+	+
I315A	-----------A----KR	17	+	+
R316A	------------A---KR	27	+	+
P317A	-------------A--KR	27	+	±
I318A	--------------A-KR	25	+	+
L319A	---------------AKR	72	+	+

binding site for 14-3-3β and ε is different from that for 14-3-3σ. Moreover, after binding to 14-3-3β or ε but not σ, CDC25B is exported to the cytoplasm. The recently published X-ray structure results revealed the following specific functional and structural features of the 14-3-3σ isoform. First, it usually forms a homodimer. Second, 14-3-3σ possesses a ligand-discriminating, special amino acid patch on the second ligand-binding surface (*38*). These findings may explain the difference in the binding properties of 14-3-3β and σ as to CDC25B.

Here, we evaluated whether four other 14-3-3 subtypes (γ, η, θ/τ, and ζ) also bind to CDC25B and exhibit behavior similar to that of 14-3-3β. The 14-3-3θ/τ isoform exhibited slightly different properties from those of the other three isoforms in that it bound to other 14-3-3 motifs in CDC25B in addition to site 309. The 14-3-3ζ isoform bound to CDC25B more weakly at Ser309 than did the other isoforms, except 14-3-3σ. These subtle differences appeared to affect the ability of these isoforms to cause the transfer of CDC25B from the nucleus to the cytoplasm. Our results show that six of the seven 14-3-3 subtypes in mammalian cells behave similarly in terms of CDC25B binding. The specific function of the 14-3-3σ isoform is unknown.

The typical consensus 14-3-3 binding sequence consists of Arg-X-X-Ser/Thr-X-P (mode-I) or Arg-X-X-X-Ser/Thr-X-P (mode-II), where the serine or threonine must be phosphorylated (*39*, *40*). In addition to these binding motifs, 14-3-3 also binds to the recently identified mode-III motif, which consists of (p)S/T-X_{1-2}-COOH at the C-terminus of several proteins (*41*). Although the results of oriented peptide analysis suggest that the Arg-X-X-(p)Ser/Thr-X-P mode-I motif is sufficient for 14-3-3 binding, a more complicated situation appears to exist *in vivo*. For example, we previously found that CDC25B contains five 14-3-3 binding motifs, but only three of these are functional. The principal 14-3-3 binding site is at Ser309, and the Ser216 site in combination with the Ser137 or Ser309 site may also be important, especially for binding to 14-3-3σ.

One possible reason for the apparent non-functionality of certain 14-3-3 binding motifs *in vivo* may be the lack of phosphorylation of target Ser/Thr. The results described in this report suggest another somewhat unexpected explanation. We found that alterations in amino acids C-terminal to the binding motif at site 309 severely impaired 14-3-3 binding, indicating that 14-3-3 binding depends not only on the consensus sequence but also on its context. Thus, the binding of 14-3-3 may require not only the presence of the binding motif in its appropriately phosphorylated form but also the presence of a suitable sequence C-terminal to the binding site. Substitution mutations of amino acid residues often disrupt the local structure of proteins. Therefore, some mutants examined in this study may harbor a structural change that abolishes 14-3-3 binding. However, Ser309 in each CDC25B mutant, except Pro317Ala, was efficiently phosphorylated at the same level as that of the wild-type protein in transfected cells. These results imply (but do not prove unequivocally) that a gross structural change should not be introduced by the mutations. Studies using an oriented peptide library with a random amino acid sequence placed C-terminal to the consensus site will be important for confirmation of our hypothesis.

The specific kinases that phosphorylate Ser309 of CDC25B have yet to be identified. We examined kinases that have been reported to phosphorylate this residue, but they exhibited essentially the same specificity toward mutated substrates *in vitro*. All of the tested kinases required a proline at residue 317 and an arginine at residue 306, although Pro317 was not essential for Ser309 phosphorylation *in vivo*. The kinase responsible for regulating CDC25B localization must exhibit an appropriate subcellular localization. In the normal cell cycle, CDC25B is located in the nucleus, and Ser309 is phosphorylated to some degree even in the absence of cellular injury (*23*). In view of this, kinases that phosphorylate Ser309 would also be expected to be located in the nucleus. Of these kinases, we propose that CHK1 and MK2 may be suitable for the phosphorylation of Ser309 of CDC25B1, even in the absence of specific cellular damage, since they are activated at low levels during DNA replication and environmental stress, respectively (Ref. *26* and our unpublished data). It is a matter for further investigation

as to whether these kinases phosphorylate this site more heavily when cells are injured.

We thank S. Elledge for the generous gift of the plasmids. This work was supported by Grants-in-Aid for Scientific Research from and by the Third-Term Comprehensive 10-Year Strategy for Cancer Control of the Ministry of Health, Labour, and Welfare of Japan. This work was also supported by the Collaborative Research Program of the Cancer Institute of Kanazawa University and by the Kanazawa University 21st Century COE Program of the Ministry of Education, Culture, Sports, Science, and Technology of Japan. S. U. was also supported by a fellowship from the Kanazawa University 21st Century COE Program and a Research-Resident Fellowship from the Human Science Foundation of Japan.

REFERENCES

1. Galaktionov, K. and Beach, D. (1991) Specific activation of cdc25 tyrosine phosphatases by B-type cyclins: evidence for multiple roles of mitotic cyclins. *Cell* **67**, 1181–1194
2. Sadhu, K., Reed, S.I., Richardson, H., and Russell, P. (1990) Human homolog of fission yeast cdc25 mitotic inducer is predominantly expressed in G2. *Proc. Natl. Acad. Sci. USA* **87**, 5139–5143
3. Strausfeld, U., Labbe, J.C., Fesquet, D., Cavadore, J.C., Picard, A., Sadhu, K., Russell, P., and Doree, M. (1991) Dephosphorylation and activation of a p34cdc2/cyclin B complex in vitro by human CDC25 protein. *Nature* **351**, 242–245
4. Jinno, S., Suto, K., Nagata, A., Igarashi, M., Kanaoka, Y., Nojima, H., and Okayama, H. (1994) Cdc25A is a novel phosphatase functioning early in the cell cycle. *EMBO J.* **13**, 1549–1556
5. Hoffmann, I., Draetta, G., and Karsenti, E. (1994) Activation of the phosphatase activity of human cdc25A by a cdk2-cyclin E dependent phosphorylation at the G1/S transition. *EMBO J.* **13**, 4302–4310
6. Kumagai, A. and Dunphy, W.G. (1992) Regulation of the cdc25 protein during the cell cycle in Xenopus extracts. *Cell* **70**, 139–151
7. Hoffmann, I., Clarke, P.R., Marcote, M.J., Karsenti, E., and Draetta, G. (1993) Phosphorylation and activation of human cdc25-C by cdc2—cyclin B and its involvement in the self-amplification of MPF at mitosis. *EMBO J.* **12**, 53–63
8. Nishijima, H., Nishitani, H., Seki, T., and Nishimoto, T. (1997) A dual-specificity phosphatase Cdc25B is an unstable protein and triggers p34(cdc2)/cyclin B activation in hamster BHK21 cells arrested with hydroxyurea. *J. Cell Biol.* **138**, 1105–1116
9. Lammer, C., Wagerer, S., Saffrich, R., Mertens, D., Ansorge, W., and Hoffmann, I. (1998) The cdc25B phosphatase is essential for the G2/M phase transition in human cells. *J. Cell Sci.* **111**, 2445–2453
10. Donzelli, M., Squatrito, M., Ganoth, D., Hershko, A., Pagano, M., and Draetta, G.F. (2002) Dual mode of degradation of Cdc25 A phosphatase. *EMBO J.* **21**, 4875–4884
11. Mailand, N., Podtelejnikov, A.V., Groth, A., Mann, M., Bartek, J., and Lukas, J. (2002) Regulation of G(2)/M events by Cdc25A through phosphorylation-dependent modulation of its stability. *EMBO J.* **21**, 5911–5920
12. Chen, M.S., Hurov, J., White, L.S., Woodford-Thomas, T., and Piwnica-Worms, H. (2001) Absence of apparent phenotype in mice lacking Cdc25C protein phosphatase. *Mol. Cell. Biol.* **21**, 3853–3861
13. Lincoln, A.J., Wickramasinghe, D., Stein, P., Schultz, R.M., Palko, M.E., De Miguel, M.P., Tessarollo, L., and Donovan, P.J. (2002) Cdc25b phosphatase is required for resumption of meiosis during oocyte maturation. *Nat. Genet.* **30**, 446–449
14. Ferguson, A.M., White, L.S., Donovan, P.J., and Piwnica-Worms, H. (2005) Normal cell cycle and checkpoint responses in mice and cells lacking Cdc25B and Cdc25C protein phosphatases. *Mol. Cell. Biol.* **25**, 2853–2860
15. Bulavin, D.V., Amundson, S.A., and Fornace, A.J. (2002) p38 and Chk1 kinases: different conductors for the G(2)/M checkpoint symphony. *Curr. Opin. Genet. Dev.* **12**, 92–97
16. Donzelli, M. and Draetta, G.F. (2003) Regulating mammalian checkpoints through Cdc25 inactivation *EMBO Rep.* **4**, 671–677
17. Bartek, J., Lukas, C., and Lukas, J. (2004) Checking on DNA damage in S phase. *Nat. Rev. Mol. Cell. Biol.* **5**, 792–804
18. Sanchez, Y., Wong, C., Thoma, R.S., Richman, R., Wu, Z., Piwnica-Worms, H., and Elledge, S.J. (1997) Conservation of the Chk1 checkpoint pathway in mammals: linkage of DNA damage to Cdk regulation through Cdc25. *Science* **277**, 1497–1501
19. Matsuoka, S., Huang, M., and Elledge, S.J. (1998) Linkage of ATM to cell cycle regulation by the Chk2 protein kinase. *Science* **282**, 1893–1897
20. O'Neill, T., Giarratani, L., Chen, P., Iyer, L., Lee, C.H., Bobiak, M., Kanai, F., Zhou, B.B., Chung, J.H., and Rathbun, G.A. (2002) Determination of substrate motifs for human Chk1 and hCds1/Chk2 by the oriented peptide library approach. *J. Biol. Chem.* **277**, 16102–16115
21. Miyata, H., Doki, Y., Yamamoto, H., Kishi, K., Takemoto, H., Fujiwara, Y., Yasuda, T., Yano, M., Inoue, M., Shiozaki, H., Weinstein, I.B., and Monden, M. (2001) Overexpression of CDC25B overrides radiation-induced G2-M arrest and results in increased apoptosis in esophageal cancer cells. *Cancer Res.* **61**, 3188–3193
22. Forrest, A. and Gabrielli, B. (2001) Cdc25B activity is regulated by 14-3-3. *Oncogene* **20**, 4393–4401
23. Bulavin, D.V., Higashimoto, Y., Popoff, I.J., Gaarde, W.A., Basrur, V., Potapova, O., Appella, E., and Fornace, A.J., Jr. (2001) Initiation of a G2/M checkpoint after ultraviolet radiation requires p38 kinase. *Nature* **411**, 102–107
24. Peng, C.Y., Graves, P.R., Thoma, R.S., Wu, Z., Shaw, A.S., and Piwnica-Worms, H. (1997) Mitotic and G2 checkpoint control: regulation of 14-3-3 protein binding by phosphorylation of Cdc25C on serine-216. *Science* **277**, 1501–1505
25. Giles, N., Forrest, A., and Gabrielli, B. (2003) 14-3-3 acts as an intramolecular bridge to regulate cdc25B localization and activity. *J. Biol. Chem.* **278**, 28580–28587
26. Manke, I.A., Nguyen, A., Lim, D., Stewart, M.Q., Elia, A.E., and Yaffe, M.B. (2005) MAPKAP kinase-2 is a cell cycle checkpoint kinase that regulates the G2/M transition and S phase progression in response to UV irradiation. *Mol. Cell* **17**, 37–48
27. Dalal, S.N., Schweitzer, C.M., Gan, J., and DeCaprio, J.A. (1999) Cytoplasmic localization of human cdc25C during interphase requires an intact 14-3-3 binding site. *Mol. Cell. Biol.* **19**, 4465–4479
28. Davezac, N., Baldin, V., Gabrielli, B., Forrest, A., Theis-Febvre, N., Yashida, M., and Ducommun, B. (2000) Regulation of CDC25B phosphatases subcellular localization. *Oncogene* **19**, 2179–2185
29. Graves, P.R., Lovly, C.M., Uy, G.L., and Piwnica-Worms, H. (2001) Localization of human Cdc25C is regulated both by nuclear export and 14-3-3 protein binding. *Oncogene* **20**, 1839–1851
30. Uchida, S., Kuma, A., Ohtsubo, M., Shimura, M., Hirata, M., Nakagama, H., Matsunaga, T., Ishizaka, Y., and Yamashita, K. (2004) Binding of 14-3-3beta but not 14-3-3sigma controls the cytoplasmic localization of CDC25B: binding site preferences of 14-3-3 subtypes and the subcellular localization of CDC25B. *J. Cell Sci.* **117**, 3011–3020
31. Furnari, B., Blasina, A., Boddy, M.N., McGowan, C.H., and Russell, P. (1999) Cdc25 inhibited in vivo and in vitro by checkpoint kinases Cds1 and Chk1. *Mol. Biol. Cell* **10**, 833–845

32. Chen, M.S., Ryan, C.E., and Piwnica-Worms, H. (2003) Chk1 kinase negatively regulates mitotic function of Cdc25A phosphatase through 14-3-3 binding. *Mol. Cell. Biol.* **23**, 7488–7497
33. Uto, K., Inoue, D., Shimuta, K., Nakajo, N., and Sagata, N. (2004) Chk1, but not Chk2, inhibits Cdc25 phosphatases by a novel common mechanism. *EMBO J.* **23**, 3386–3396
34. Guan, K.L. and Dixon, J.E. (1991) Eukaryotic proteins expressed in Escherichia coli: an improved thrombin cleavage and purification procedure of fusion proteins with glutathione S-transferase. *Anal. Biochem.* **192**, 262–267
35. Wang, X., Arooz, T., Siu, W.Y., Chiu, C.H., Lau, A., Yamashita, K., and Poon, R.Y. (2001) MDM2 and MDMX can interact differently with ARF and members of the p53 family. *FEBS Lett.* **490**, 202–208
36. Bradford, M.M. (1976) A rapid and sensitive method for the quantitation of microgram quantities of protein utilizing the principle of protein-dye binding. *Anal. Biochem.* **72**, 248–254
37. Uchida, S., Ohtsubo, M., Shimura, M., Hirata, M., Nakagama, H., Matsunaga, T., Yoshida, M., Ishizaka, Y., and Yamashita, K. (2004) Nuclear export signal in CDC25B. *Biochem. Biophys. Res. Commun.* **316**, 226–232
38. Wilker, E.W., Grant, R.A., Artim, S.C., and Yaffe, M.B. (2005) A structural basis for 14-3-3sigma functional specificity. *J. Biol. Chem.* **280**, 18891–18898
39. Muslin, A.J., Tanner, J.W., Allen, P.M., and Shaw, A.S. (1996) Interaction of 14-3-3 with signaling proteins is mediated by the recognition of phosphoserine. *Cell* **84**, 889–897
40. Yaffe, M.B., Rittinger, K., Volinia, S., Caron, P.R., Aitken, A., Leffers, H., Gamblin, S.J., Smerdon, S.J., and Cantley, L.C. (1997) The structural basis for 14-3-3:phosphopeptide binding specificity. *Cell* **91**, 961–971
41. Ganguly, S., Weller, J.L., Ho, A., Chemineau, P., Malpaux, B., and Klein, D.C. (2005) Melatonin synthesis: 14-3-3-dependent activation and inhibition of arylalkylamine N-acetyltransferase mediated by phosphoserine-205. *Proc. Natl. Acad. Sci. USA* **102**, 1222–1227

Inhibition of peroxisome proliferator-activated receptor gamma activity in esophageal carcinoma cells results in a drastic decrease of invasive properties

Hirokazu Takahashi,[1] Kouji Fujita,[1] Toshio Fujisawa,[1] Kyoko Yonemitsu,[1] Ayako Tomimoto,[1] Ikuko Ikeda,[1] Masato Yoneda,[1] Tomotaka Masuda,[2] Katherine Schaefer,[3] Lawrence J Saubermann,[3] Takeshi Shimamura,[1] Satoru Saitoh,[1] Masashi Tachibana,[4] Koichiro Wada,[2] Hitoshi Nakagama[4] and Atsushi Nakajima[1,5]

[1]Gastroenterology Division, Yokohama City University Graduate School of Medicine, 3-9 Fukuura, Kanazawa-ku, Yokohama, Kanagawa 236-0004; [2]Department of Pharmacology, School of Dentistry, Osaka University, 1-8 Yamadaoka, Suita, Osaka 565-0871, Japan; [3]Section of Gastroenterology, Boston University School of Medicine, Boston, MA, USA; and [4]Biochemistry Division, National Cancer Center Research Institute, 5-1-1 Tsukiji, Chuo-ku, Tokyo 104-0045, Japan

(Received December 19, 2005/Revised April 24, 2006/Accepted May 1, 2006/Online publication June 29, 2006)

Esophageal cancer is difficult to treat because of its rapid progression, and more effective therapeutic approaches are needed. The PPARγ is a nuclear receptor superfamily member that is expressed in many cancers. PPARγ expression is a feature of esophageal cancer cell lines, and in the present investigation, the PPARγ antagonists T0070907 and GW9662 could induce loss of invasion but could not induce growth reduction or apoptosis at low concentrations (<10 mM). A high concentration of antagonists (50 μM) inhibited cell growth and induced apoptosis, but these effects did not explain our result at the low concentration. Morphological change, decreased expression of the cell signaling pathway and inhibition of cancer cell invasion were observed in the low concentration. This suggested that PPARγ antagonists inhibited esophageal cancer cell invasion as well as cell adherence, most likely due to alteration in the FAK–MAPK pathway, and this was independent of apoptosis. These results suggested that PPARγ plays an important role in cancer cell invasion and that it might be a novel target for therapy of esophageal cancer. (*Cancer Sci* 2006; 97: 854–860)

Esophageal cancer is associated with a high mortality rate due to its typically late presentation and rapid progression. For tumors that are not amenable to surgical curative resection, chemotherapy and radiotherapy are commonly applied. But most patients continue to have a poor prognosis, along with an increased morbidity due to treatment-related side-effects.[1] Clearly, new therapies for esophageal cancer are needed.

The nuclear transcription factor PPARγ has recently become a putative therapeutic cancer target for a variety of cancers.[2–4] As PPARγ is mainly expressed in adipose tissue and activation plays a central role in adipocyte differentiation and insulin sensitivity,[5] activating synthethic ligands, TZDs, are commonly used as oral antihyperglycemic agents in control of diabetes mellitus type 2. However, PPARγ is also overexpressed in many tumors, including examples in the esophagus, stomach, breast, lung and colon, suggesting that modulation of PPARγ function might impact on tumor survival.[2–4,6,7] Initial efforts have focused on activation with the TZD ligands, as these have been shown to induce G1 cell cycle arrest in a variety of tumor cell lines.[8,9] However, the results of clinical trials with TZDs have shown modest, if any, benefit.[10,11] With esophageal cancers, PPARγ activation by TZDs in cell lines has been reported to inhibit *in vitro* cell growth and/or induce apoptosis.[12–14]

Several observations suggest that inhibition of PPARγ function might be beneficial in treating neoplasms.[15,16] PPARγ is overexpressed in many cancer cell types, but loss-of-function mutations are rare,[17] suggesting that the receptor is a tumor cell survival factor. The hypothesis that PPARγ function might contribute to carcinogenesis or cancer cell survival is also supported by the observation that in one murine model of colon cancer, PPARγ activation led to an increase in tumor formation.[18,19]

Little is known about inhibition of PPARγ function in esophageal cancer cells. In this study, we investigated the effect of PPARγ inhibition on esophageal cancer cell lines using PPARγ-specific antagonists T0070907 and GW9662 in high (50 μM), low (<10 μM) and very low (<10 μM) concentrations. The PPARγ antagonist could prevent cell attachment to the ECM in high concentrations in our previous studies, however, the effect of PPARγ antagonists in low concentrations was not clear.[20,21] A better understanding of the PPARγ function might lead to it being further utilized for cancer treatment.

Materials and methods

Reagents

The PPARγ-specific antagonists T0070907 and GW9662 were purchased from Cayman Chemical (Ann Arbor, MI, USA) and Sigma Chemical (St Louis, MO, USA), respectively.

[5]To whom correspondence should be addressed.
E-mail: nakajima-tky@umin.ac.jp

Abbreviations: DMEM, Dulbecco's minimum essential medium; ECM, extracellular matrix; Erk, extracellular signal-regulated kinase; FAK, focal adhesion kinase; FITC, fluorescein-isothiocyanate; MAPK, mitogen-activated protein kinase; MTT, 3-(4,5-dimethylthiazol-2-yl)-2,5-diphenyltetrazolium bromide; p-Erk, phosphorylated extracellular signal-regulated kinase; p-FAK, phosphorylated focal adhesion kinase; PPARγ, peroxisome proliferator-activated receptor gamma; TZDs, thiazolizinediones.

doi: 10.1111/j.1349-7006.2006.00250.x

Cell culture

Human esophageal cancer cells (KYSE30, KYSE70, KYSE140) used in this study were obtained from the Human Science Foundation (Osaka, Japan). The histology of KYSE30 was well differentiated, KYSE70 poorly, and KYSE140 moderately. KYSE30 and KYSE70 were maintained in DMEM and KYSE140 in Ham's F12 supplemented with 2% fetal bovine serum. Cultures were maintained at 37°C, with an atmosphere of 5% CO_2 and saturated humidity.

Western blot analysis

Adherent cells were washed in phosphate-buffered saline, and cell extracts were prepared in Laemmli lysis buffer. Protein concentrations were measured using Bio-Rad Protein Assay Reagent (Bio-Rad, Richmond, CA, USA) following the manufacturer's suggested procedure. After electrophoresis of 20 μg aliquots using 10% sodium dodecylsulfate–polyacrylamide gel electrophoresis, proteins were transferred to nitrocellulose membranes (Millipore, Bedford, MA, USA), blocked for 1 h in tris-buffered saline with bovine serum albumin at room temperature, and incubated with primary monoclonal antibody for 1 h. The anti-PPARγ antibody (E-8) was purchased from Santa Cruz Biotechnology (Santa Cruz, CA, USA), anti-pFAK(pY397) from BD Biosciences (San Jose, CA, USA) and anti-p-Erk from Cellsignaling Technology (Beverly, MA, USA). After three washings, the membranes were incubated for 1 h at room temperature with secondary antibody, and immune complexes were visualized using the enhanced chemiluminescence detection kit (Amersham, London, UK) following the manufacturer's procedure.

Immunofluorescence and cell morphology

Cells (5×10^5 per well) were grown on collagen-1 coated glass cover slips in six-well flat bottom plates for 24 h. T0070907 and GW9662 were added and the cells were pre-incubated for 24 h. The cells were fixed with 4% formaldehyde followed by 100% ethanol at −20°C. Permeabilization was carried out with 0.1% Triton-X, and non-specific binding was blocked with 2% normal swine serum. Cells were incubated with antipaxillin monoclonal antibody (BD Biosciences) followed by FITC-labeled secondary antibody. Alexa fluoro 594-conjugated phalloidin (Molecular Probes, Eugene, OR, USA) was used to visualize F-actin. The samples were then mounted with Vectashield (Vector Laboratories, Burlingame, CA, USA) and examined by confocal laser scanning microscopy (Carl Zeiss, Oberkochen, Germany). All experiments were done in triplicate.

Assessment of cell growth

Cell proliferation was measured by MTT assay.[22] KYSE70 cells were plated in 96-well plates at a concentration of 5×10^3 cells in 100 μL of DMEM. After 24 h incubation, the medium was changed with various concentrations of T0070907 and GW9662 added (1–50 μM), and the cells further incubated for 24–72 h. MTT solution (0.5%) was then added to each well. After the plates were incubated for 4 h, 20% sodium dodecylsulfate solution was incubated and absorbance at 595 nm was determined using a microplate reader (Model 550; Bio-Rad). Control wells were treated with dimethylsulfoxide alone. Three independent experiments were carried out.

Apoptosis assay

To evaluate the apoptotic cell death, annexin V staining was carried out using an annexin V–FITC apoptosis detection kit I (Becton Dickinson, San Jose, CA, USA) according to the manufacturer's recommendations. Cells were subsequently analyzed by FACScan flow cytometry (Becton Dickinson).

Transwell invasion assays

In vitro cell invasion was assayed in BD BioCoat Matrigel invasion chambers (24 wells, 8 μm pore size; BD Biosciences). The top chamber was seeded with 5×10^4 KYSE70 cells in DMEM. The bottom chamber was filled with DMEM supplemented with 2% fetal bovine serum as a chemoattractant. Cells were preincubated with T0070907 and GW9662 (1–10 μM) in the top chamber, followed by incubation for 24 h in a humidified tissue culture incubator at 37°C under a 5% CO_2 atmosphere. Noninvasive cells were removed from the upper surface of the membrane with a cotton swab, and cells on the lower surface of the membrane were fixed and stained with toluidine blue and mounted on glass slides. Five random fields/well were counted for quantitation of cell invasion. Triplicate wells were counted for each assay.

Statistical analysis

All results are expressed as means ± standard errors of the mean. Statistical comparisons were made using either Student's *t*-test or Scheffe's method after ANOVA. Differences were considered significant at $P < 0.05$.

Results

Esophageal cancer expresses PPARγ protein

Human esophageal cancer tissues were stained using anti-PPARγ-specific antibody, and the expression was high in area of cancer invasion (Fig. 1a). To test whether inhibiting PPARγ activity affects esophageal cell growth or survival, three esophageal cell lines, KYSE30, KYSE70 and KYSE140, were examined. Western blot analysis revealed differential PPARγ protein expression in each. The expression level of PPARγ was very low in normal mucosa, low in KYSE30 cells (well differentiated), moderate in KYSE140 cells (moderately differentiated) and high in KYSE70 cells (poorly differentiated). As the degree of cell differentiation decreased from well differentiated to poorly differentiated, PPARγ protein expression increased. The expression of PPARγ was increased in esophageal cancer tissues compare with normal esophageal epithelial cells (Fig. 1b). The cell line with the highest expression of PPARγ, KYSE70, was used in subsequent investigations into the inhibitory effect of PPARγ activity.

Treatment with PPARγ antagonists decreases cell adhesion to the ECM

Cells treated with 10 or 50 μM of T0070907 and GW9662 underwent morphological changes by 24 h, but those treated with 1 μM did not undergo any morphological change (Fig. 2). At this time point, most cells were still adherents to the plate. However, rather than becoming the normal elongated shape, they were rounded. This morphological change was not the result of apoptosis in cells treated with

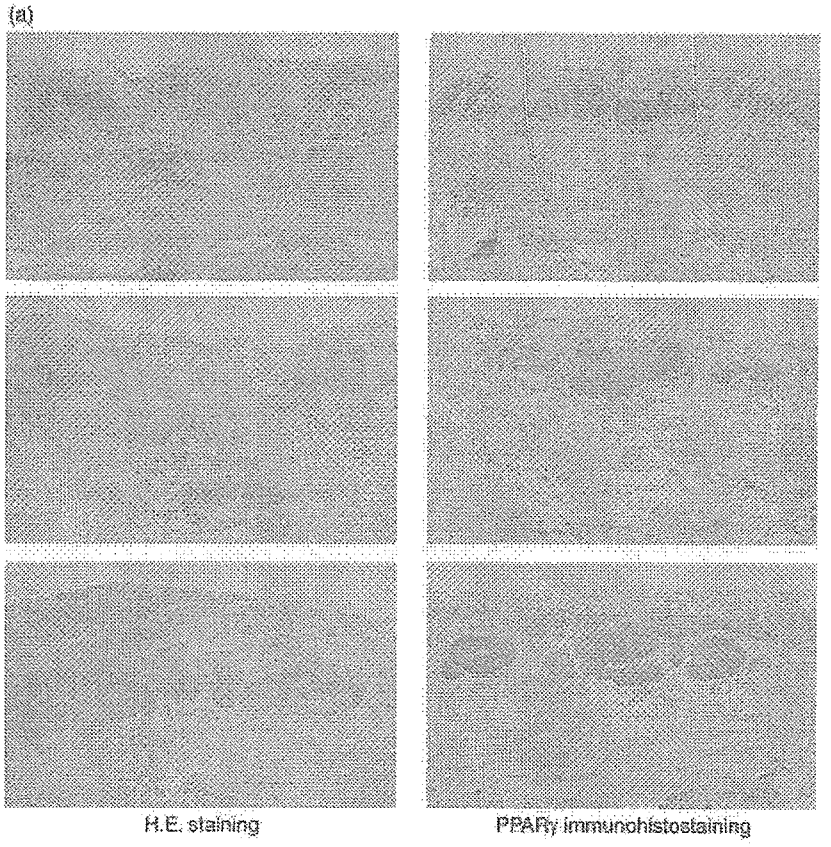

Fig. 1. PPARγ expression in esophageal cancer. (a) Surgical resection of human esophageal cancer tissue stained using HE and antibody specific for PPARγ. The expression was high in area of cancer invasion. (b) The expression level of PPARγ was very low in normal mucosa, low in KYSE30 cells (well differentiated), moderate in KYSE140 cells (moderately differentiated) and high in KYSE70 cells (poorly differentiated). As the degree of cell differentiation decreased from well differentiated to poorly differentiated, PPARγ protein expression increased.

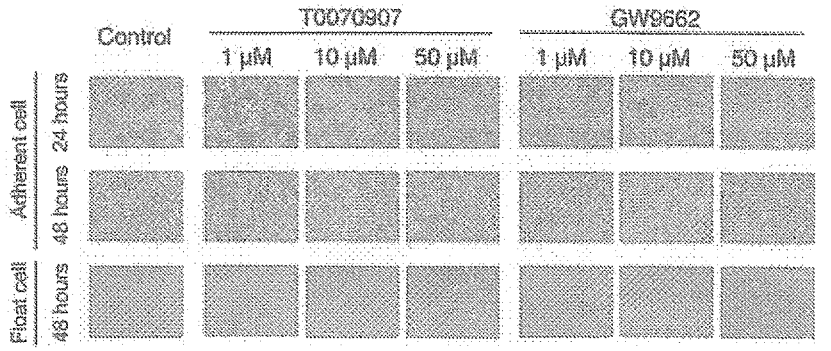

Fig. 2. Morphological changes in esophageal cancer cell lines induced by PPARγ antagonists. KYSE70 cells were incubated with dimethylsulfoxide (control), and 1–50 μM T0070907 and GW9662. Cells treated with 10 and 50 μM of PPARγ antagonists underwent morphological changes by 24 h. By 48 h, 10 μM induced morphological changes but did not inhibit cell adherence; 50 μM induced morphological changes and inhibited cell adherence.

10 μM T0070907 and GW9662, as cells at this time point were not positive for annexin V (Fig. 3). By 48 h, almost half of the cells treated with 50 μM T0070907 and GW9662 were nonadherent. In other words, 1 μM of antagonists induced no change, 10 μM induced morphological changes but did not inhibit cell adherence, and 50 μM induced morphological changes and inhibited cell adherence.

PPARγ antagonists induce change of actin organization

Actin fibers play an important role in maintaining the cytoskeletal structure, and paxillin is functionally important in transducing intracellular messages that are associated with growth factor signaling and cell–ECM interactions.[23] To determine whether the observed cell rounding was associated with alterations in cytoskeletal function, these proteins were

doi: 10.1111/j.1349-7006.2006.00250.x

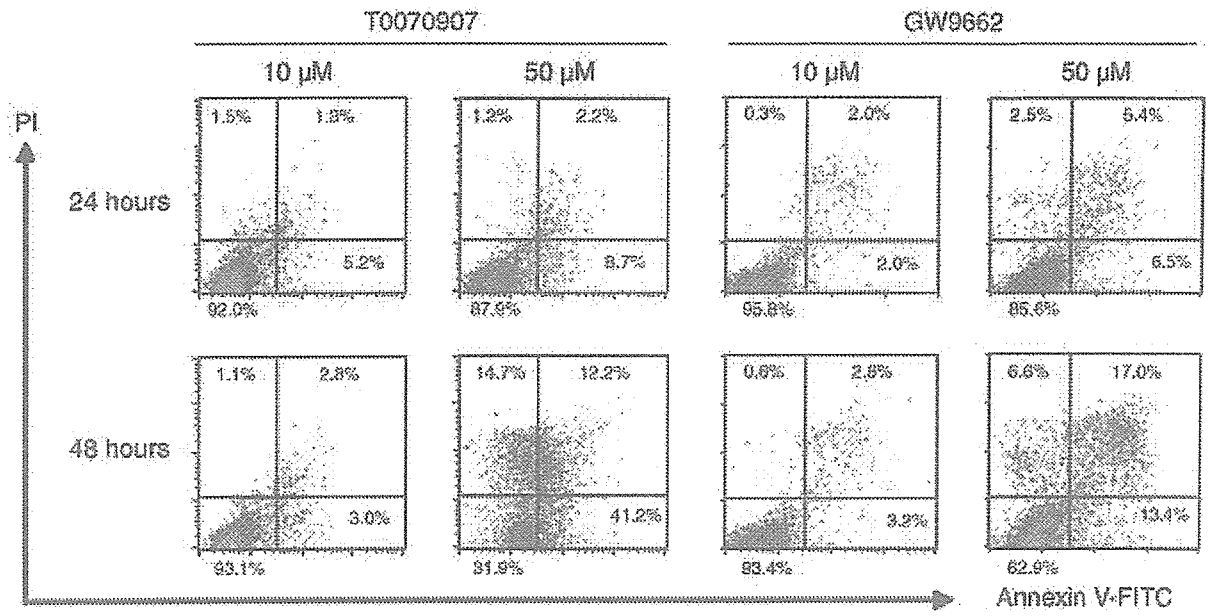

Fig. 3. PPARγ antagonists induced apoptosis in KYSE70 esophageal cancer cells at 48 h. Cells were incubated with 10 and 50 μM T0070907 and GW9662, followed by flow cytometry analysis using annexin V and propidium iodide double staining. Apoptotic cells were observed in 50 μM antagonists at the 48 h time point, but not in 10 μM.

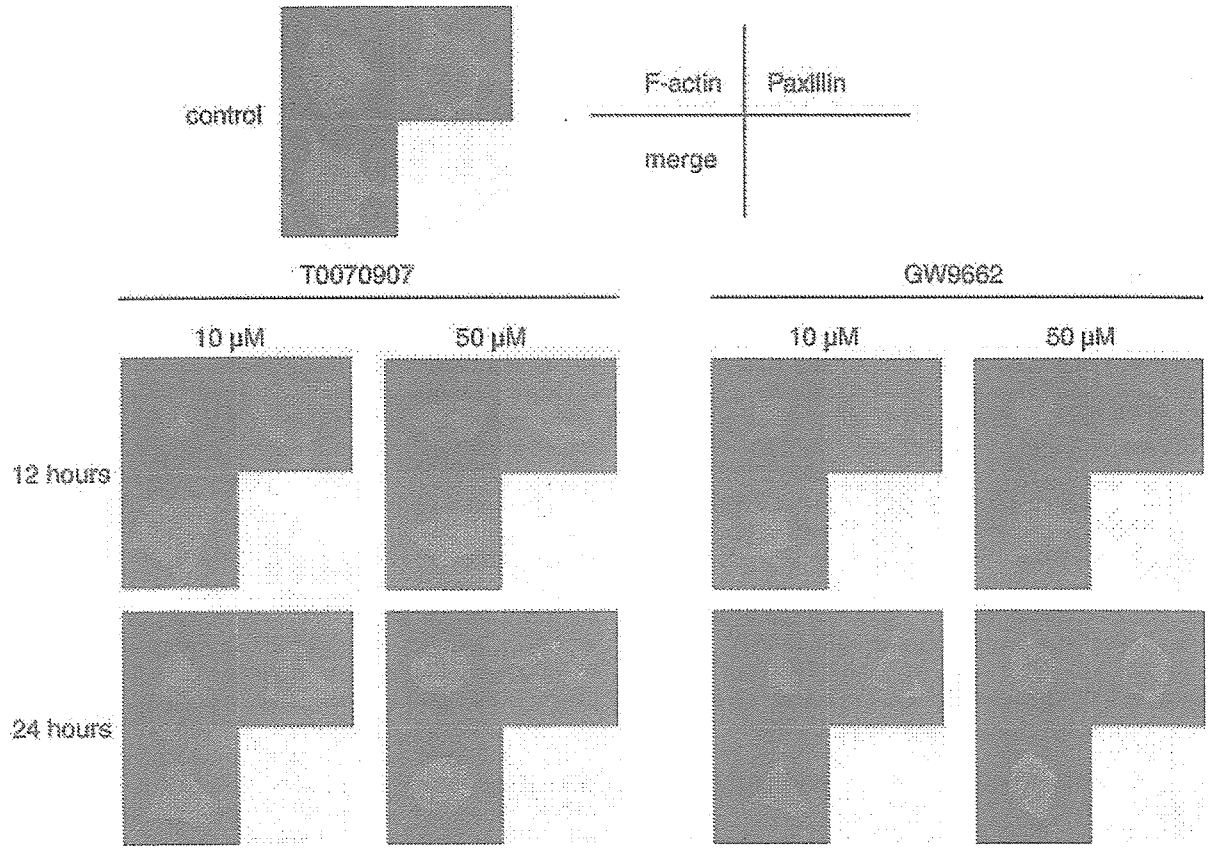

Fig. 4. Before PPARγ antagonist treatment of KYSE70 esophageal cancer cells, actin fibers and paxillin were visible. After 12 h of treatment with 10 and 50 μM T0070907 and GW9662, the cells began to lose their actin fibers, and by 24 h almost all of the cells had changed to a round shape with complete loss of actin fibers.

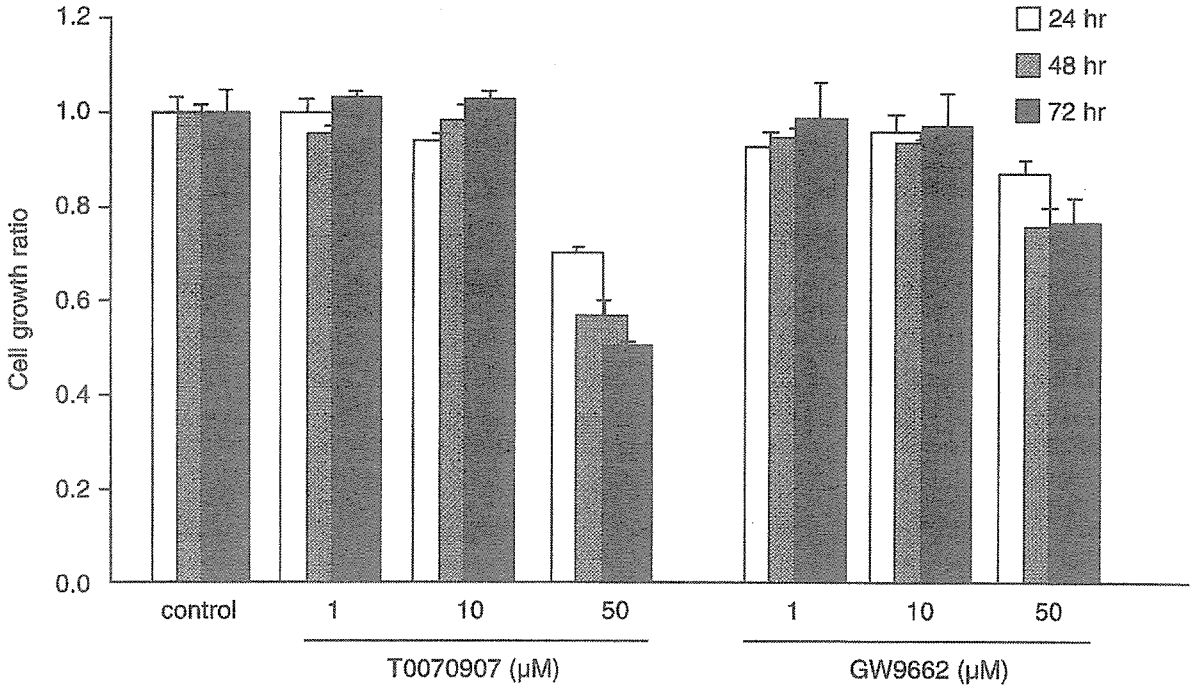

Fig. 5. The PPARγ antagonists T0070907 and GW9662 prevented cell growth in KYSE70 esophageal cancer cells. MTT assay showed the cell growth ratio was significantly reduced in cells treated with 50 μM PPARγ antagonists, and this effect was time-dependent. PPARγ antagonists at concentrations below 10 μM did not reduce the cell growth ratio.

examined by confocal microscopy. Before antagonist treatment, actin fibers and paxillin were visible (Fig. 4). After 12 h of treatment in 10 and 50 μM PPARγ antagonists, the cells began to lose their actin fibers, and by 24 h almost all the KYSE70 cells had changed to a round shape with loss of actin fibers. Similar results were obtained with KYSE30 and KYSE140 cells (data not shown).

Effect of PPARγ antagonists on cell growth

In order to compare the effects of PPARγ antagonism on esophageal cancer cell growth, KYSE70 cells were incubated with T0070907 and GW9662. At 24, 48 and 72 h, the number of cells was measured using MTT assay (Fig. 5). The results were similar in all cell lines, therefore we used KYSE70 cells because they had the highest expression of PPARγ. The compounds did not reduce the growth ratio at concentrations below 10 μM, but did at 50 μM.

Effect of PPARγ antagonists on apoptotic cell death

The results of propidium iodide–annexin V–FITC staining showed that the PPARγ-specific antagonists both induced apoptosis in KYSE70 cells by 48 h at a concentration of 50 μM (Fig. 3), but did not induce apoptosis at 10 μM.

PPARγ antagonism affects the ability of esophageal cancer cell invasion

The PPARγ antagonists had the potential to decrease cell invasiveness. In transwell invasion assays, the number of invasive KYSE70 cells significantly decreased with antagonist treatment below 10 μM, and this effect dose-dependent (Fig. 6). At this concentration (10 μM), the PPARγ antagonists did not induce apoptosis, suggesting that the effect of invasion reduction was independent of apoptosis.

PPARγ antagonism inhibits the phosphorylation of FAK and Erk

To determine possible mechanisms of the cell growth inhibition by PPARγ antagonism, important adhesion and survival cell signaling pathways were investigated. PPARγ antagonists altered FAK (Tyr397) and Erk phosphorylation. KYSE70 cells were incubated with 10 μM of each antagonist.

The results of Western blot analysis revealed decreased expression of p-FAK and p-Erk by the treatment with the antagonists (Fig. 7). p-FAK decreased after 9 h and p-Erk decreased after 12 h.

Discussion

Currently, there is very little information about the inhibition of PPARγ in cancer cells, including esophageal cancer cells. Our previous studies using hepatocellular carcinoma and tongue cancer cells have demonstrated that PPARγ antagonists (high concentration, 50 μM) could prevent cell attachment to ECM, leading to loss of adhesion-induced apoptosis.[20,21] Tongue and esophageal cancer are similar in that they are both squamous cell carcinomas, but the treatment approaches are different. However, esophageal cancer is clinically very important because its mortality rate is very high.

In this study, we demonstrated using esophageal cancer cells that a very low concentration (<10 μM) of PPARγ

doi: 10.1111/j.1349-7006.2006.00250.x

antagonists could induce the inhibition of invasive properties, but not induce growth reduction or apoptosis. MTT assay (Fig. 5) showed that a low and very low concentration of PPARγ antagonists did not inhibit the growth ratio, even after 72 h. Similarly, a low concentration (10 μM) of PPARγ antagonists did not induce apoptosis (Fig. 3). However, a low concentration of PPARγ antagonists could inhibit the cancer cell invasion in the transwell migration assays (Fig. 6). These results suggested that the mechanism by which the PPARγ antagonists inhibited the cancer cell invasion at low concentrations was different from the mechanism by which the high concentration induced apoptosis and cell growth reduction. Therefore, our results suggested that PPARγ might play an important role in cancer cell invasion.

Several reports have clearly demonstrated that PPARγ agonist ligands, the TZDs, could inhibit cell growth and apoptosis of adenocarcinomas, as well as esophageal cancer tissues.[14,24–26] The PPARγ antagonists T0070907 and GW9662 could induce a very similar inhibition of cell growth at a high concentration (50 μM) (Fig. 4). Although it appears paradoxical that both over-activation and inhibition of PPARγ activity could lead to reduced cell growth, this might be a result of different mechanisms. In the TZD setting, a well-recognized G0–G1 cell cycle arrest occurs. In contrast, with PPARγ antagonists, apoptosis appeared to follow loss of adhesion, which was not observed using TZDs. It is suggested that both PPARγ antagonists and TZDs should be considered important candidates for further development as anticancer agents.

PPARγ antagonists were found to first affect cell morphology, with almost all cells changing their cytoskeletal structure, involving both actin fibers and paxillin, within the first 12 h. After adopting a rounded shape, the cells then began detaching from the ECM by 24 h. At this time point, the cells were clearly not apoptotic, as determined by flow cytometric analysis in low concentration (10 μM). This suggested there were different mechanisms dependent on PPARγ activity.

FAK, a 125 kDa non-receptor tyrosine kinase, is an important regulator of cell survival, invasion, migration, and cell cycle

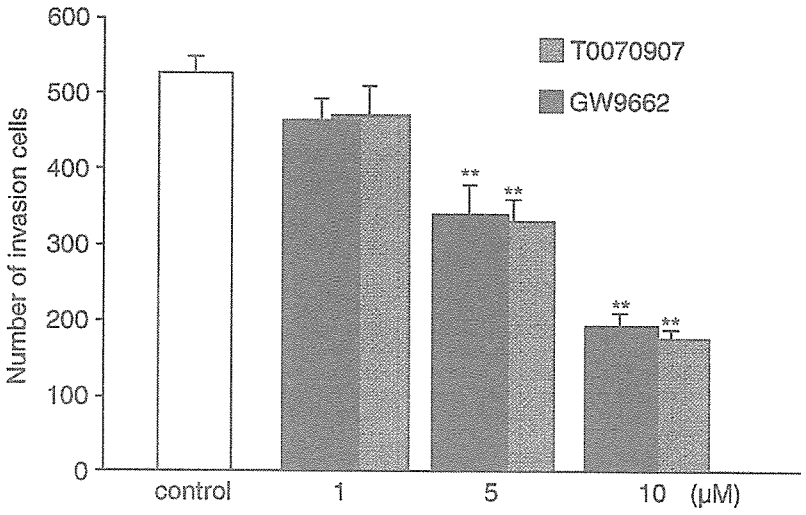

Fig. 6. KYSE70 esophageal cancer cells were incubated with PPARγ antagonists for 24 h during a transwell invasion assay. The number of invasive cells was decreased with antagonist treatment below 10 μM, and this effect was dose-dependent. Error bars represent standard errors of the mean for three replicates. *$P < 0.05$, **$P < 0.01$.

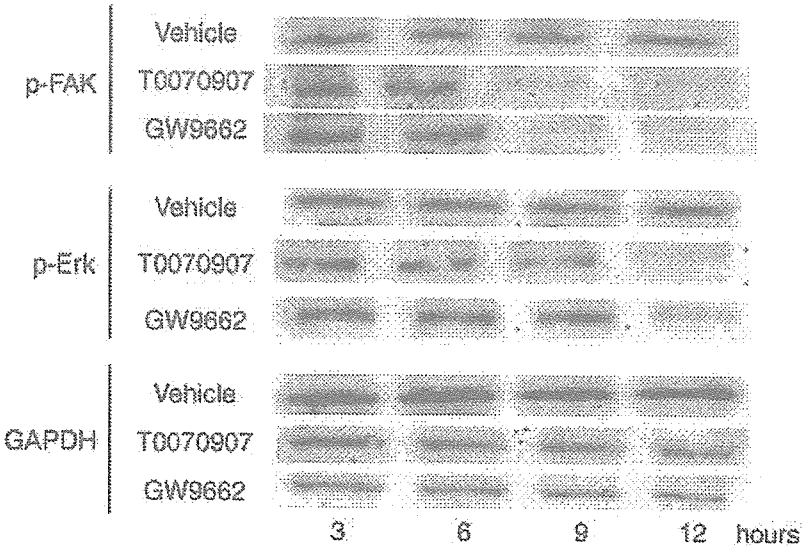

Fig. 7. Expression of FAK (Tyr397) and Erk phosphorylation was altered in KYSE70 esophageal cancer cells incubated with 10 μM PPARγ antagonists. p-FAK was decreased at 9 h and p-Erk was decreased at 12 h.

progression.[27–29] This overexpression of FAK has been observed in a number of human malignant cells, and this might play an important role in determining cellular invasion and metastasis.[30,31] FAK is functionally important in transducing intracellular messages associated with growth factor signaling, cell–ECM interactions, modifying the cytoskeleton and activating MAPK cascades, including Erk. In the present study, the inhibition of phosphorylation of FAK in KYSE70 cells treated with antagonists (10 μM) was observed at 9 h, followed by a reduction in Erk phosphorylation at 12 h. Inhibition of Erk phosphorylation occurred after the inhibition of FAK phosphorylation by PPARγ antagonists, suggesting that PPARγ might play an important role in the MAPK pathway.

High concentration (50 μM) PPARγ antagonists induced apoptosis and cell detachment, and reduced cell growth, but a low concentration (10 μM) could reduce cell invasion and alter the MAPK signaling pathway. These results suggest that the effects of a low concentration of antagonists were independent of the effects of apoptosis, detachment and cell growth inhibition. One study has reported that the difference in effect depends on PPARγ concentration,[32] but further investigation is necessary.

In summary, PPARγ antagonists inhibited esophageal cancer cell invasion as well as cell adherence to ECM, most likely due to alteration in the FAK–MAPK pathway, and this was independent of apoptosis. Our results suggest that PPARγ plays important roles in cancer cell invasion, therefore it might be a novel target for esophageal cancer therapy.

Acknowledgments

This work was supported by a Grants-in-Aid for the Third Term Comprehensive Control Research for Cancer from the Ministry of Health, Labour, and Welfare of Japan, and the Ministry of Education, Science, Sports, Culture, Japan.

References

1 Blazeby JM, Alderson D, Farndon JR. Quality of life in patients with oesophageal cancer. *Recent Results Cancer Res* 2000; **155**: 193–204.
2 Takashima T, Fujiwara Y, Higuchi K *et al.* PPAR-gamma ligands inhibit growth of human esophageal adenocarcinoma cells through induction of apoptosis, cell cycle arrest and reduction of ornithine decarboxylase activity. *Int J Oncol* 2001; **19**: 465–71.
3 Chang TH, Szabo E. Induction of differentiation and apoptosis by ligands of peroxisome proliferator-activated receptor gamma in non-small cell lung cancer. *Cancer Res* 2000; **60**: 1129–38.
4 DuBois RN, Gupta R, Brockman J, Reddy BS, Krakow SL, Lazar MA. The nuclear eicosanoid receptor, PPARgamma, is aberrantly expressed in colonic cancers. *Carcinogenesis* 1998; **19**: 49–53.
5 Desvergne B, Wahli W. Peroxisome proliferator-activated receptors: nuclear control of metabolism. *Endocr Rev* 1999; **20**: 649–88.
6 Mueller E, Sarraf P, Tontonoz P *et al.* Terminal differentiation of human breast cancer through PPAR gamma. *Mol Cell* 1998; **1**: 465–70.
7 Sato H, Ishihara S, Kawashima K *et al.* Expression of peroxisome proliferator-activated receptor (PPAR) gamma in gastric cancer and inhibitory effects of PPARgamma agonists. *Br J Cancer* 2000; **83**: 1394–400.
8 Guan YF, Zhang YH, Breyer RM, Davis L, Breyer MD. Expression of peroxisome proliferator-activated receptor gamma (PPARgamma) in human transitional bladder cancer and its role in inducing cell death. *Neoplasia* 1999; **1**: 330–9.
9 Kitamura S, Miyazaki Y, Shinomura Y, Kondo S, Kanayama S, Matsuzawa Y. Peroxisome proliferator-activated receptor gamma induces growth arrest and differentiation markers of human colon cancer cells. *Jpn J Cancer Res* 1999; **90**: 75–80.
10 Debrock G, Vanhentenrijk V, Sciot R, Debiec-Rychter M, Oyen R, Van Oosterom A. A phase II trial with rosiglitazone in liposarcoma patients. *Br J Cancer* 2003; **89**: 1409–12.
11 Kulke MH, Demetri GD, Sharpless NE *et al.* A phase II study of troglitazone, an activator of the PPARgamma receptor, in patients with chemotherapy-resistant metastatic colorectal cancer. *Cancer J* 2002; **8**: 395–9.
12 Hashimoto Y, Shimada Y, Itami A *et al.* Growth inhibition through activation of peroxisome proliferator-activated receptor gamma in human oesophageal squamous cell carcinoma. *Eur J Cancer* 2003; **39**: 2239–46.
13 Fujii D, Yoshida K, Tanabe K, Hihara J, Toge T. The ligands of peroxisome proliferator-activated receptor (PPAR) gamma inhibit growth of human esophageal carcinoma cells through induction of apoptosis and cell cycle arrest. *Anticancer Res* 2004; **24**: 1409–16.
14 Rumi MA, Sato H, Ishihara S, Ortega C, Kadowaki Y, Kinoshita Y. Growth inhibition of esophageal squamous carcinoma cells by peroxisome proliferator-activated receptor-gamma ligands. *J Lab Clin Med* 2002; **140**: 17–26.
15 Martelli ML, Iuliano R, Le Pera I *et al.* Inhibitory effects of peroxisome poliferator-activated receptor gamma on thyroid carcinoma cell growth. *J Clin Endocrinol Metab* 2002; **87**: 4728–35.
16 Panigrahy D, Shen LQ, Kieran MW, Kaipainen A. Therapeutic potential of thiazolidinediones as anticancer agents. *Expert Opin Invest Drugs* 2003; **12**: 1925–37.
17 Posch MG, Zang C, Mueller W *et al.* Somatic mutations in peroxisome proliferator-activated receptor-gamma are rare events in human cancer cells. *Med Sci Monit* 2004; **10**: BR250–254.
18 Lefebvre AM, Chen I, Desreumaux P *et al.* Activation of the peroxisome proliferator-activated receptor gamma promotes the development of colon tumors in C57BL/6J-APCMin/+ mice. *Nat Med* 1998; **4**: 1053–7.
19 Saez E, Tontonoz P, Nelson MC *et al.* Activators of the nuclear receptor PPARgamma enhance colon polyp formation. *Nat Med* 1998; **4**: 1058–61.
20 Schaefer KL, Wada K, Takahashi H *et al.* Peroxisome proliferator-activated receptor gamma inhibition prevents adhesion to the extracellular matrix and induces anoikis in hepatocellular carcinoma cells. *Cancer Res* 2005; **65**: 2251–9.
21 Masuda T, Wada K, Nakajima A *et al.* Critical role of peroxisome proliferator-activated receptor gamma on anoikis and invasion of squamous cell carcinoma. *Clin Cancer Res* 2005; **11**: 4012–21.
22 Mosmann T. Rapid colorimetric assay for cellular growth and survival: application to proliferation and cytotoxicity assays. *J Immunol Meth* 1983; **65**: 55–63.
23 Giancotti FG, Ruoslahti E. Integrin signaling. *Science* 1999; **285**: 1028–32.
24 Eibl G, Wente MN, Reber HA, Hines OJ. Peroxisome proliferator-activated receptor gamma induces pancreatic cancer cell apoptosis. *Biochem Biophys Res Commun* 2001; **287**: 522–9.
25 Ohta K, Endo T, Haraguchi K, Hershman JM, Onaya T. Ligands for peroxisome proliferator-activated receptor gamma inhibit growth and induce apoptosis of human papillary thyroid carcinoma cells. *J Clin Endocrinol Metab* 2001; **86**: 2170–7.
26 Shimada T, Kojima K, Yoshiura K, Hiraishi H, Terano A. Characteristics of the peroxisome proliferator activated receptor gamma (PPARgamma) ligand induced apoptosis in colon cancer cells. *Gut* 2002; **50**: 658–64.
27 Chen HC, Appeddu PA, Parsons JT, Hildebrand JD, Schaller MD, Guan JL. Interaction of focal adhesion kinase with cytoskeletal protein talin. *J Biol Chem* 1995; **270**: 16995–9.
28 Sieg DJ, Hauck CR, Ilic D *et al.* FAK integrates growth-factor and integrin signals to promote cell migration. *Nat Cell Biol* 2000; **2**: 249–56.
29 Schaller MD. Biochemical signals and biological responses elicited by the focal adhesion kinase. *Biochim Biophys Acta* 2001; **1540**: 1–21.
30 Agochiya M, Brunton VG, Owens DW *et al.* Increased dosage and amplification of the focal adhesion kinase gene in human cancer cells. *Oncogene* 1999; **18**: 5646–53.
31 Owens LV, Xu L, Dent GA *et al.* Focal adhesion kinase as a marker of invasive potential in differentiated human thyroid cancer. *Ann Surg Oncol* 1996; **3**: 100–5.
32 Yamauchi T, Waki H, Kamon J *et al.* Inhibition of RXR and PPARgamma ameliorates diet-induced obesity and type 2 diabetes. *J Clin Invest* 2001; **108**: 1001–13.

doi: 10.1111/j.1349-7006.2006.00250.x

Carcinogenesis vol.27 no.1 pp.162–169, 2006
doi:10.1093/carcin/bgi205
Advance Access publication August 4, 2005

Strain differences in the susceptibility to azoxymethane and dextran sodium sulfate-induced colon carcinogenesis in mice

Rikako Suzuki*, Hiroyuki Kohno, Shigeyuki Sugie, Hitoshi Nakagama[1] and Takuji Tanaka

Department of Oncologic Pathology, Kanazawa Medical University, 1-1 Daigaku, Uchinada, Ishikawa 920-0293, Japan and [1]Biochemistry Division, National Cancer Center Research Institute, 5-1-1 Tsukiji Chuo-ku, Tokyo 104-0045, Japan

*To whom correspondence should be addressed. Tel: +81 76 286 2211; Fax: +81 76 286 6926; E-mail: rikako@kanazawa-med.ac.jp

We have recently developed a mouse model for colitis-related colon carcinogenesis by a combined treatment with azoxymethane (AOM) and dextran sodium sulfate (DSS) in male ICR mice. However, strain differences in the sensitivity to AOM/DSS-induced colon carcinogenesis in mice have yet to be elucidated. The aim of this study was to determine the presence of any genetically determined differences in sensitivity to our model of colon carcinogenesis in four inbred strains of mice. Male Balb/c, C3H/HeN, C57BL/6N and DBA/2N mice were given a single intraperitoneal injection of AOM (10 mg/kg body wt), followed by 1% DSS (w/v) in drinking water for 4 days, and thereafter they received no further treatment for up to 16 weeks. At the end of the study (Week 18), all mice were killed and a histopathological analysis of their colon was performed. The incidence of colonic adenocarcinoma was 100% with a multiplicity (no. of tumors/mouse) of 7.7 ± 4.3 in the Balb/c mice and 50% with a multiplicity of 1.0 ± 1.2 in the C57BL/6N mice. On the other hand, only a few colonic adenomas, but no adenocarcinomas, developed in the C3H/HeN mice (29% incidence with a multiplicity of 0.7 ± 1.5) and the DBA/2N mice (20% incidence with a multiplicity of 0.2 ± 0.4). The inflammation and immunohistochemical nitrotyrosine-positivity scores of the mice treated with AOM and DSS in the decreasing order were as follows: C3H/HeN > Balb/c > DBA/2N > C57BL/6N and Balb/c > C57BL/6N > C3H/HeN > DBA/2N, respectively. Our results thus indicated the presence of strain differences in the susceptibility to AOM/DSS-induced colonic tumorigenesis. These differences may have been directly influenced by the response to nitrosation stress due to the inflammation caused by DSS.

Introduction

Colorectal cancer (CRC) is one of the most common malignant neoplasms in both sexes (1). In Western countries, this malignancy is one of the most leading causes of cancer deaths (1). In patients with inflammatory bowel disease (IBD), including ulcerative colitis (UC) and Crohn's disease, the risk of CRC development is higher than in the general population (2–5). In sporadic and IBD-related CRC, the expression of inducible nitric oxide synthase and cyclooxygenase-2, both of which are associated with inflammation, has been reported to be elevated (6,7). As a result, inflammation is suggested to play an important role in IBD-related CRC (2).

In our recent series of studies on inflammation-related colon carcinogenesis, we developed a novel model of colitis-related colon carcinogenesis using ICR mice. In this animal model, ICR mice received a single dose of a different colonic carcinogen, consisting of either azoxymethane (AOM) (8), 2-amino-1-methyl-6-phenylimidazo[4,5-*b*]pyridine (9) or 1, 2-dimethylhydrazine (10), followed by a 1-week exposure to 2% dextran sodium sulfate (DSS) in their drinking water, which thus resulted in a high incidence of colonic epithelial malignancy within 20 weeks (8–10). We have previously proposed that the colonic inflammation and nitrosative stress caused by DSS exposure contributes to the development of cryptal dysplasia and neoplasms in the colon (8–10).

AOM is a colonic genotoxic carcinogen that is extensively used for the investigation of large bowel carcinogenesis in rodents (11–13). A synthetic sulfate polysaccharide, DSS, is a non-genotoxic colonic carcinogen that is widely used to produce colitis in rodents, which shares most features with human UC (14–18). It is well known that different strains of mice have different sensitivities to xenobiotic including AOM and DSS (19–28). For example, the Balb/CJ strain is known to be susceptible to AOM (26), whereas, the C3H (29), C57BL/6J (26) and DBA/2 (25) strains are less sensitive to AOM. Regarding the sensitivity to DSS in several mouse strains, Balb/c, C3H/HeJ, and C57BL/6J mice are relatively susceptible to DSS, while DBA/2J mice have been reported to be virtually resistant (27,28). It may therefore be possible that the differences in the genetic background of the mice differently affect the colon carcinogenesis induced by AOM and DSS.

The current study was conducted to determine the different sensitivities to AOM/DSS-induced colon carcinogenesis in four different inbred mouse strains, namely Balb/c, C3H/HeN, C57BL/6N and DBA/2N, by evaluating the incidence and multiplicity of colonic tumors. In addition, an immunohistochemical analysis of nitrotyrosine, a marker of both formation of peroxynitrite (30) and perhaps the inflammation-associated carcinogenesis (31), was done to evaluate whether nitrosative stress is involved in the strain difference sensitivity to AOM/DSS-induced colon tumorigenesis.

Materials and methods

Animals, chemicals and diets

For the study 5-week-old male mice of Balb/c, C3H/HeN, C57BL/6N and DBA/2N strains were obtained from Charles River Japan, (Tokyo, Japan). AOM was purchased from the Sigma-Aldrich (St Louis, MO). DSS with a molecular weight of 36 000–50 000 was purchased from ICN Biochemicals,

Abbreviations: AOM, azoxymethane; CRC, colorectal cancer; CYP, Cytochrome P450; DSS, dextran sodium sulfate; IBD, inflammatory bowel disease; IKK, IκB kinase; LPS, lipopolysaccharide; UC, ulcerative colitis.

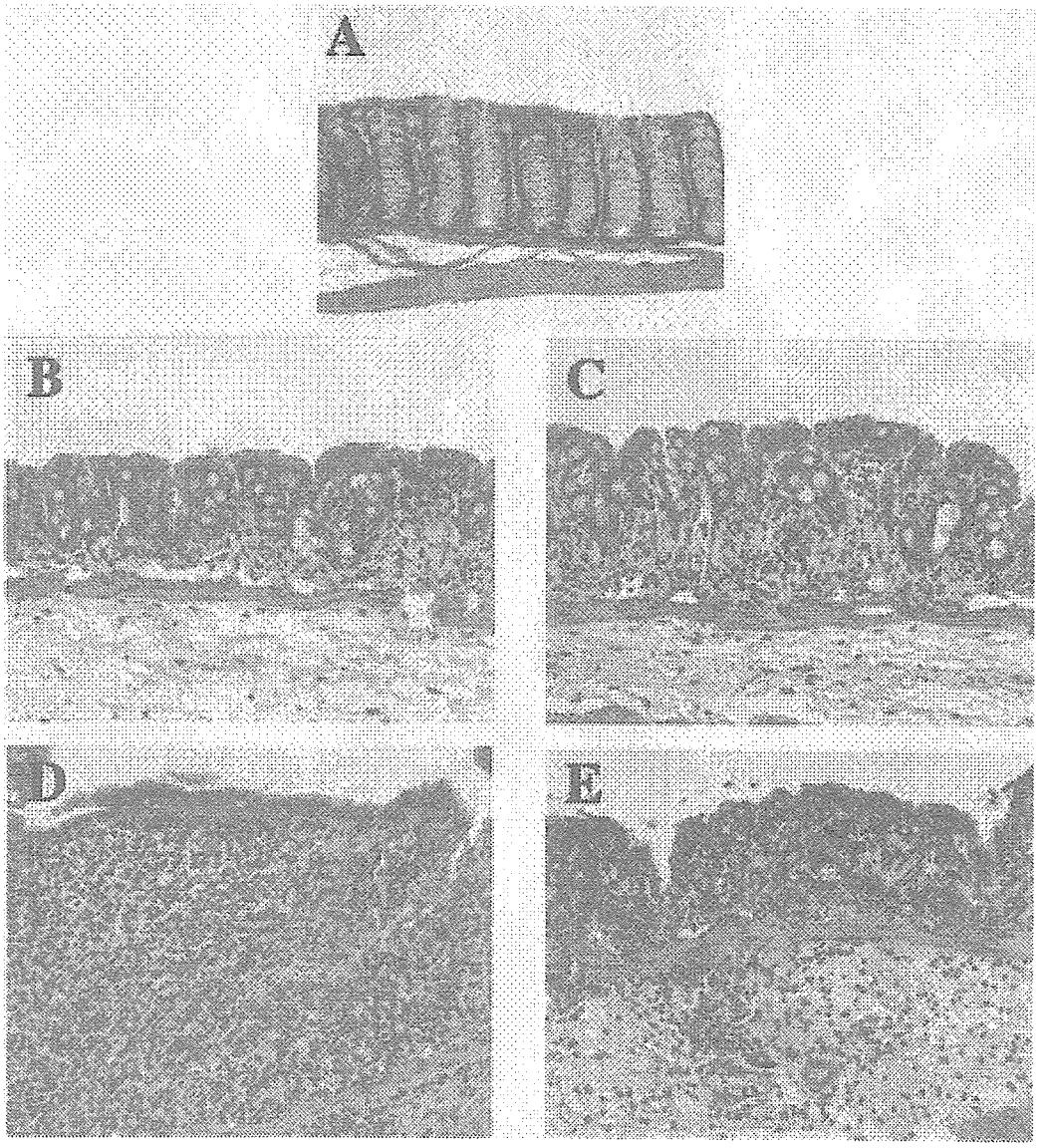

Fig. 1. Various grades of colitis. (A) Normal colon mucosa (Grade 0); (B) shortening the basal one-third of the crypts with slight inflammation and edema in the lamina propria (Grade 1); (C) loss of the basal two-thirds of the crypts with moderate inflammation in the lamina propria (Grade 2); (D) loss of all the crypts with severe inflammation in the lamina propria, but with the surface epithelium still remaining (Grade 3); and (E) a loss of all the crypts and surface epithelium with severe inflammation in the mucosa, muscularis propria and submucosa. An exudate containing cell debris, inflammatory cells, fibrin and mucus covers the damaged mucosa (Grade 4). Hematoxylin and eosin stain. Original magnification, (A–E), 20×.

(Cat. No. 160110, Aurora, OH). CRF-1 (Oriental Yeast, Tokyo, Japan) was used as the basal diet throughout the study.

Experimental procedure

After they were brought, the mice were acclimated for 1 week with tap water and a pelleted basal diet, CRF-1, *ad libitum*. The experimental groups in each strain of mice included the AOM and DSS group, the AOM alone group, the DSS alone group and the untreated control group. The experimental protocol in the current study was slightly modified from our original protocol (8). We chose 1% as the dose level of DSS since this dose has been shown to exert sufficient tumor-promoting effects (32). In addition, the duration (4 days) of DSS exposure in drinking water was shortened based on our preliminary investigation, in which 4 days of exposure to DSS was found to enhance AOM-initiated colon carcinogenesis in ICR mice of either sex. All mice were maintained at the Kanazawa Medical University Animal Facility according to the Institutional Animal Care Guidelines, and were maintained under controlled conditions of humidity (50 ± 10%), light (12/12 h light/dark cycle) and temperature (23 ± 2°C).

Histopathological analysis

At the end of the experiment (Week 18), all the mice were killed by an ether overdose. At autopsy, their large bowel was flushed with saline and excised. After measuring the length of the large bowel (from the ileocecal junction to the anal verge), it was cut open longitudinally along the main axis and washed with saline. The large bowel was then carefully inspected for the presence of pathological lesions and fixed in 10% buffered formalin for at least 24 h. Paraffin-embedded sections of the large bowel were then made by routine procedures. Any histopathological alterations in the colon were examined on hematoxylin and eosin-stained sections. Colitis was recorded and scored according to the following morphological criteria described by Cooper *et al.* (33): Grade 0 (Figure 1A), normal colonic mucosa; Grade 1 (Figure 1B), shortening and loss of the basal one-third of the actual crypts with mild inflammation and edema in the mucosa; Grade 2 (Figure 1C), loss of the basal two-thirds of the crypts with moderate inflammation in the mucosa; Grade 3 (Figure 1D), loss of all crypts with severe inflammation in the mucosa, but with the surface epithelium still remaining; and Grade 4 (Figure 1E), loss

of all crypts and the surface epithelium with severe inflammation in the mucosa, muscularis propria and submucosa. Intestinal neoplasms were diagnosed according to the criteria described by Pozharisski (34).

Immunohistochemistry

Nitrotyrosine immunohistochemistry was carried out on 4-μm-thick paraffin-embedded sections from the colons in all four strains of mice administered 1% DSS alone as previously described (8,35). The deparaffinized sections were incubated overnight with a primary rabbit polyclonal anti-nitrotyrosine (diluted 1:1500, CHEMICON International, CA) or with a control solution. Control sections included buffer alone or non-specific purified rabbit secondary antibody and avidin–biotin-peroxidase complex (Vectastain Elite ABC kit, Vector Laboratories, Burlingame, CA). The color was developed using 3,3′-diaminobenzidine-4HCl as the chromogen. The stained sections were examined for the localization and intensity of immunoreactivity by microscopy (Olympus AX70, Olympus Optical, Tokyo, Japan). To the degree of nitrotyrosine stainability, the following grading system (Grade 0–4) was applied: Grade 0, no immunoreactivity and no positive cells; Grade 1, weak immunoreactivity and <10% positive cells; Grade 2, mild immunoreactivity and 10–30% positive cells; Grade 3, moderate immunoreactivity and 31–60% positive cells; and Grade 4, strong immunoreactivity and 61–100% positive cells with extensive immunoreactivity (36).

Statistical analysis

Where applicable, the data were analyzed using one-way ANOVA with either Bonferroni correction or Fisher's exact probability test (GraphPad Instat version 3.05, GraphPad Software, San Diego, CA), with $P < 0.05$ as the criterion of significance.

Results

General observation

The intake of DSS-containing tap water did not significantly differ among the four strains of mice (data not shown). Mice that received AOM and 1% DSS or 1% DSS alone demonstrated bloody stools either during DSS administration or soon after the cessation of DSS exposure. The degree of this symptom varied among the strains: Balb/c and C3H/HeN mice showed severe symptoms while C57BL/6N and DBA/2N mice showed mild symptoms. The mean body weight and colon length of the mice are summarized in Table I. The mean body weight of the Balb/c mice, which received AOM/DSS, was significantly lower than that of the C3H/HeN mice ($P < 0.01$) and C57BL/6N mice ($P < 0.01$), which were given AOM and DSS. A significant difference on the mean body weight was found between the AOM/DSS group and the untreated group ($P < 0.001$) in Balb/c mice. As listed in Table I, the mean lengths of the colon in the Balb/c mice ($P < 0.001$) and C3H/HeN mice ($P < 0.001$) that were treated with AOM/DSS were statistically longer than in the C57BL/6N mice. A significant difference ($P < 0.001$) was also observed between the C57BL/6N and DBA/2N mice that were exposed to AOM/DSS. The C57BL/6N mice given AOM alone has a significantly shorter colon than the Balb/c ($P < 0.01$) and DBA/2N mice ($P < 0.01$) treated with AOM alone. As for the untreated group, the colon length of the C57BL/6N mice was significantly shorter than that of the Balb/c ($P < 0.01$) and DBA/2N mice ($P < 0.01$).

Incidence and multiplicity of large bowel neoplasms

Macroscopically, colonic neoplasms developed with a different incidence and multiplicity for each strain of mice that received AOM and 1% DSS. Flat, nodular, polypoid or caterpillar-like tumors were mainly located in the middle and/or distal colon if any tumors existed (Figure 2). Histopathologically, they were tubular adenoma (Figure 3A) or adenocarcinoma (Figure 3B). Dysplastic lesions were also observed in the colonic mucosa surrounding the tumors. None of the strains of mice given AOM alone, 1% DSS alone or tap water had any colonic tumors.

Table I. Body and relative liver weights and lengths of colon in each strain of mice

Strain	Treatment (no. of mice examined)	Body weight (g)	Length of colon (cm)
Balb/c	AOM→1% DSS (10)	25.1 ± 3.8[a,b,c,d]	12.7 ± 1.0[e]
	AOM (4)	30.9 ± 0.8	14.0 ± 1.0[f]
	1% DSS (5)	34.1 ± 2.0	13.0 ± 0.6
	None (5)	32.4 ± 1.1	13.7 ± 0.5[g]
C3H/HeN	AOM→1% DSS (7)	30.2 ± 0.6	12.7 ± 1.3[e]
	AOM (5)	32.6 ± 2.2	12.5 ± 0.6
	1% DSS (5)	32.2 ± 1.2	13.1 ± 1.1
	None (3)	31.8 ± 1.1	11.9 ± 0.6
C57BL/6N	AOM→1% DSS (10)	29.3 ± 1.9	11.1 ± 0.6[h]
	AOM (5)	31.3 ± 2.0	11.7 ± 0.5[i]
	1% DSS (5)	32.0 ± 1.7	12.8 ± 0.9
	None (5)	33.0 ± 4.7	11.6 ± 1.0[j]
DBA/2N	AOM→1% DSS (10)	28.3 ± 2.3	13.2 ± 1.0
	AOM (5)	28.9 ± 1.3	14.1 ± 0.9
	1% DSS (5)	30.5 ± 0.6	14.0 ± 0.8
	None (5)	30.7 ± 1.4	13.6 ± 1.7

[a]Mean ± SD.
[b]Significantly different from untreated Balb/c mice ($P < 0.001$).
[c]Significantly different from C3H/HeN mice which received AOM/DSS ($P < 0.01$).
[d]Significantly different from C57BL/6N mice which received AOM/DSS ($P < 0.01$).
[e]Significantly different from C57BL/6N mice which received AOM/DSS ($P < 0.001$).
[f]Significantly different from C57BL/6N mice which received AOM alone ($P < 0.01$).
[g]Significantly different from untreated C57BL/6N mice ($P < 0.01$).
[h]Significantly different from DBA/2N mice which received AOM/DSS ($P < 0.001$).
[i]Significantly different from DBA/2N mice which received AOM alone ($P < 0.01$).
[j]Significantly different from untreated DBA/2N mice ($P < 0.01$).

The incidence (percent of mice with tumors) of colonic neoplasms is summarized in Figure 4A. The incidence of colonic neoplasms in the Balb/c mice (100%) was significantly higher than in the C3H/HeN mice (29%, $P = 0.0034$) and the DBA/2N mice (20%, $P = 0.0004$). A statistically significant difference ($P = 0.0115$) was also noted between the C57BL/6N (80%) and the DBA/2N mice. The order of the incidence of colonic adenoma was Balb/c mice (90%) > C57BL/6N mice (70%) > C3H/HeN mice (29%) > DBA/2N mice (20%). The incidence of adenoma in Balb/c mice was statistically greater than in C3H/HeN mice ($P = 0.0175$) and DBA/2N mice ($P = 0.0027$), and the difference between C57BL/6N mice and DBA/2N mice was statistically significant ($P = 0.0349$). The incidence of colonic adenocarcinoma was 100% in the Balb/c mice and 50% in the C57BL/6N mice and a statistically significant difference ($P = 0.0163$) was found between these two strains of mice. However, this malignancy was not found in the C3H/HeN and DBA/2N mice. As shown in Figure 4B, the multiplicity of colonic neoplasms (/mouse) was 11.4 ± 5.9 in Balb/c mice, 0.7 ± 1.5 in C3H/HeN mice, 2.5 ± 2.1 in C57BL/6N mice and 0.2 ± 0.4 in DBA/2N mice. The value for the Balb/c mice was significantly higher ($P < 0.001$) than that of other strains of mice. The order of the multiplicity of adenoma was Balb/c mice (3.7 ± 3.3) > C57BL/6N mice (1.5 ± 1.3) > C3H/HeN mice (0.7 ± 1.5) > DBA/2N mice (0.2 ± 0.4). The value for multiplicity of adenoma in the Balb/c mice was statistically greater than in the C3H/HeN

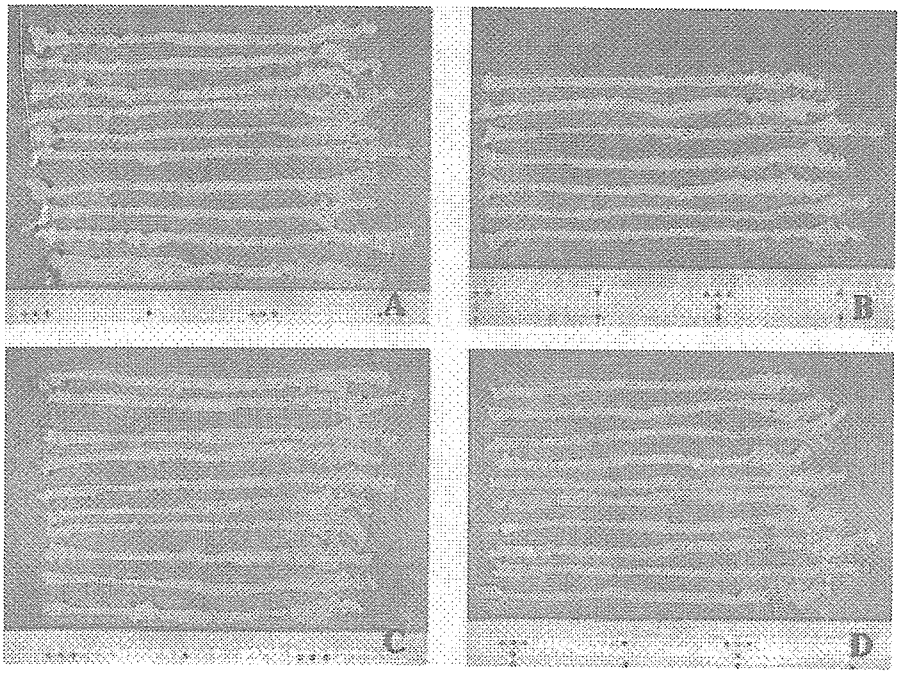

Fig. 2. Macroscopic view of the large bowel treated with AOM and 1% DSS. (A) Numerous colon tumors (2–21 tumors per mouse) develop in all Balb/c mice. (B) One or four colonic tumors are seen in two out of seven C3H/HeN mice. (C) One to five colonic tumors are found in 8 out of 10 C57BL/6N mice. (D) One colonic tumor is present in 2 out of 10 DBA/2N mice.

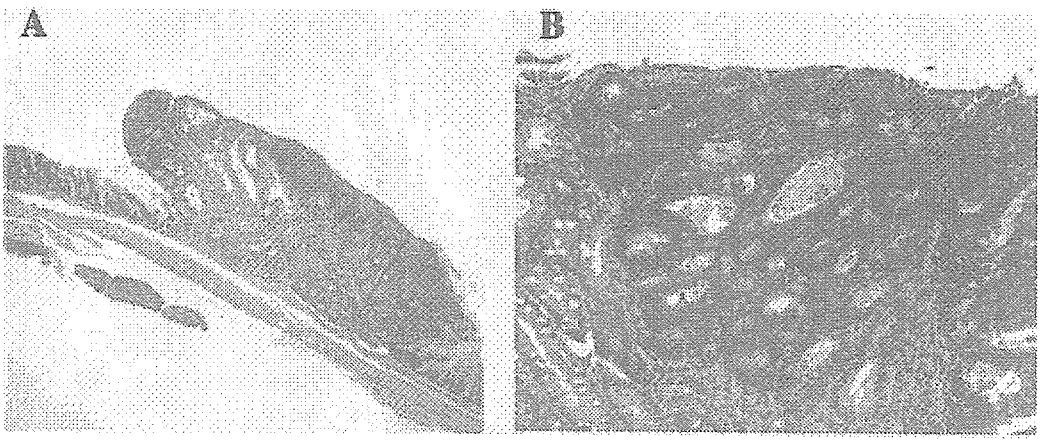

Fig. 3. Histopathology of colonic neoplasms in male Balb/c mice treated with AOM and 1% DSS. (A) Tubular adenoma and (B) moderately-differentiated adenocarcinoma. Hematoxylin and eosin stain. Original magnification, A, 2× and B, 20×.

mice ($P < 0.05$) and DBA/2N mice ($P < 0.01$). The multiplicity of adenocarcinoma in the Balb/c mice (7.7 ± 4.3) was the greatest among the four strains and it was significantly larger than that in the C3H/HeN mice (1.0 ± 1.2, $P < 0.001$).

The scores of inflammation and nitrotyrosine

As shown in Figure 5, the inflammation scores of each strain of mice initiated with AOM and followed by DSS exposure were 1.2 ± 1.1 in Balb/c, 2.3 ± 1.3 in C3H/HeN, 0.4 ± 0.7 in C57BL/6N and 0.6 ± 0.7 in DBA/2N, respectively. The score of C3H/HeN was significantly greater than that for C57BL/6N ($P<0.01$) and DBA/2N ($P<0.01$). As for the mice that received 1% DSS alone, the inflammation score of the C3H/HeN mice (1.4 ± 0.5) was the highest among the strains (1.0 ± 1.2 in Balb/c mice and 0.2 ± 0.4 in DBA/2N mice). C57BL/6N mice given 1% DSS alone had quite a low score of inflammation. The mice treated with AOM alone and the untreated mice demonstrated extremely weak inflammation in the colon.

Nitrotyrosine immunoreactivity was mainly observed in the neoplastic cells, cryptal cells, blood endothelial cells and mononuclear cells, which infiltrated the colonic mucosa (Figure 6). The stainability was relatively weak for infiltrative mononuclear cells in comparison with the cryptal cells and endothelial cells (Figure 6). As shown in Figure 7, the nitrotyrosine immunohistochemistry findings for the Balb/c mice (3.6 ± 0.5) treated with AOM and DSS were significantly higher than those for C3H/HeN (1.7 ± 0.8, $P<0.001$) and DBA/2N mice (1.6 ± 0.5, $P<0.001$). The score of nitrotyrosine-positivity in C57BL/6N mice (3.4 ± 0.5) was

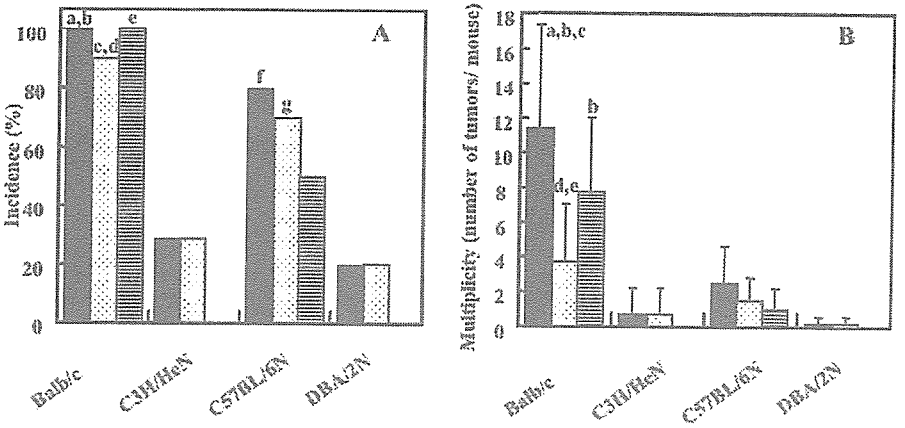

Fig. 4. Incidence and multiplicity of colonic tumors. (A) Incidence of colonic tumors. Black columns represent total; white column filled with dots represent adenoma and striped columns represent adenocarcinoma. a, Significantly different from C3H/HeN (P=0.0034); b, significantly different from DBA/2N (P = 0.0004); c, significantly different from C57BL/6N (P=0.0175); d, significantly different from DBA/2N (P=0.0027); e, significantly different from C57BL/6N (P=0.0163); f, significantly different from DBA/2N (P=0.0115); and g, significantly different from DBA/2N (P=0.0349). (B) Multiplicity of colonic tumors. Values are the mean ± SD. Black columns represent total; white column filled with dots represent adenoma and striped columns represent adenocarcinoma. a, Significantly different from C3H/HeN (P < 0.001); b, significantly different from C57BL/6N (P < 0.001); c, significantly different from DBA/2N (P < 0.001); d, significantly different from C3H/HeN (P < 0.05); and e, significantly different from DBA/2N (P < 0.01).

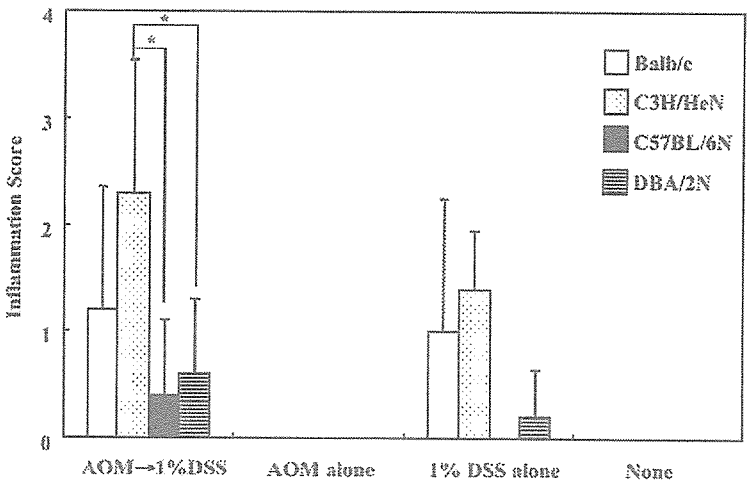

Fig. 5. Inflammation score in the colon for four strains of mice. Values are the mean ± SD. white column, Balb/c; white column with dots, C3H/HeN; black columns, C57BL/6N; striped columns, DBA/2N. *P < 0.01.

statistically higher than those in C3H/HeN (P < 0.001) and DBA/2N (P < 0.001) mice. In mice that received 1% DSS alone, the scores in Balb/c (2.8 ± 0.8) and C57BL/6N (2.4 ± 1.1) mice were higher than those in C3H/HeN (1.6 ± 0.5) and DBA/2N mice (1.4 ± 0.5); however, no significant differences were observed among the strains. As for the mice given AOM alone, the scores of nitrotyrosine in the Balb/c mice and C57BL/6N mice were 0.5 ± 0.6 and 0.2 ± 0.4, respectively. C3H/HeN mice and DBA/2N mice treated with AOM alone showed either no or faint stainability of nitrotyrosine. The degree of nitrotyrosine stainability in untreated mice was almost null.

Discussion

The present investigation demonstrated the different susceptibilities of the four strains (Balb/c, C3H/HeN, C57BL/6N and DBA/2N) of mice to colon tumorigenesis induced by the combination treatments with AOM and DSS. Apparently, Balb/c mice were extremely sensitive to AOM/DSS-induced colon carcinogenesis in the present experimental condition. The sensitivity of Balb/c mice observed in the present study was almost similar to those found in ICR mice (8,32,35). Colonic adenocarcinoma also developed in C57BL/6N, but the incidence was lower than in Balb/c. In contrast, the susceptibility of C3H/HeN and DBA/2N to the administration of AOM and DSS was quite low and only a few colonic adenomas developed in both the strains of mice.

Regarding the sensitivity of the mice to AOM initiation, the Balb/CJ mice were reported to have a remarkable susceptibility to the formation of distal colon tumors after treatment with AOM (26), whereas C3H, C57BL/6J, and DBA/2 mice were found to have a low incidence of colonic tumors by AOM initiation (25,26,29). Strain differences in the susceptibility to DSS have also been demonstrated: Balb/c, C3H/HeJ and C57BL/6J are relatively susceptible to DSS, whereas DBA/2J mice are virtually resistant based on the frequency of ulceration or the histological score of inflammation in the colon

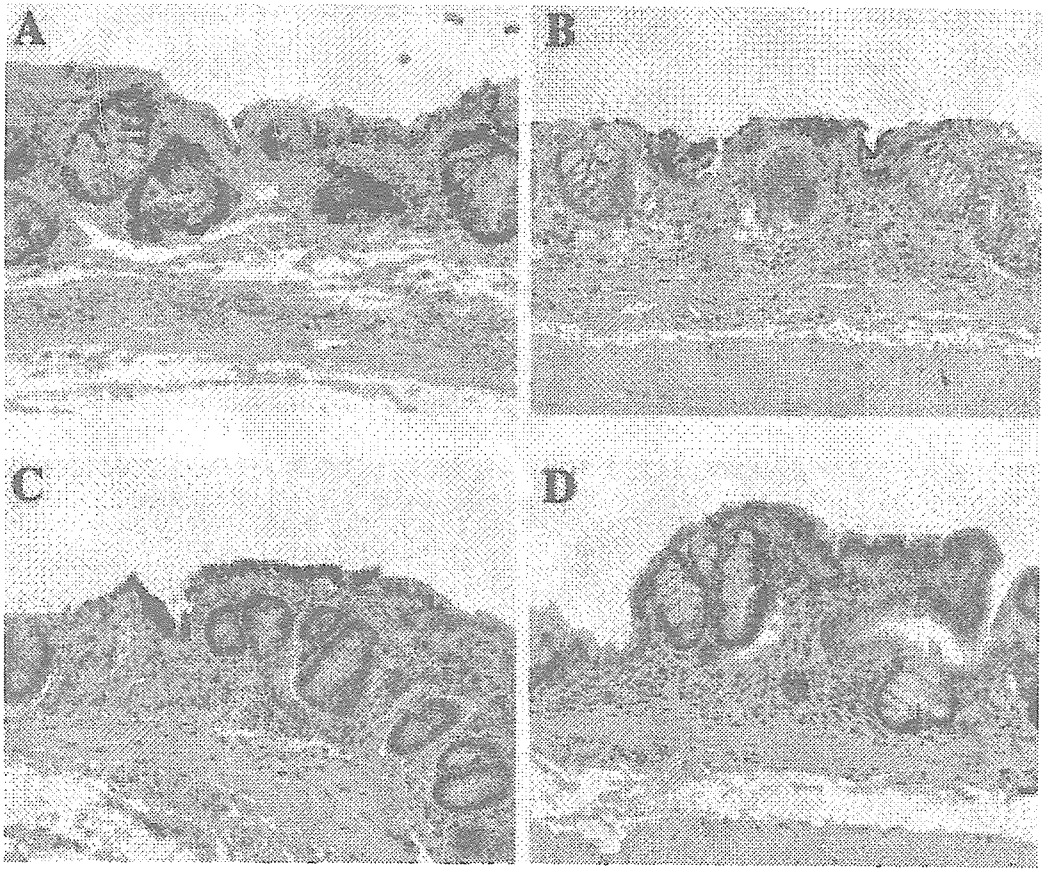

Fig. 6. Nitrotyrosine immunohistochemistry of the colon from four strains of mice given 1% DSS. (A) Balb/c; (B) C3H/HeN; (C) C57BL/6N; and (D) DBA/2N.Original magnification, (A–D), 20×.

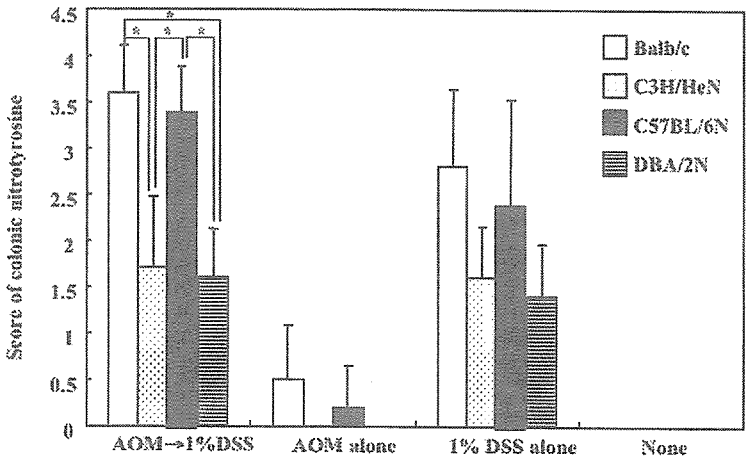

Fig. 7. Score for nitrotyrosine immunohistochemistry. Values are the mean ± SD. White column, Balb/c; white column with dots, C3H/HeN; black columns, C57BL/6N; striped columns, DBA/2N. *$P < 0.001$.

(27,28). In the current study, the sensitivities of the four strains to DSS were somewhat dissimilar to those of previous studies (27,28). The inflammation score of colonic mucosa revealed a severe and moderate inflammation to be present in the C3H/HeN and Balb/c mice treated with both AOM and DSS, respectively, while C57BL/6N and DBA/2N mice had only a relatively weak inflammation. In the case of the receptivity of C57BL mice to lipopolysaccharide (LPS), C57BL/10ScCr mice were resistant to LPS, whereas C57BL/10ScSn mice responded to LPS (37). Similarly, C3H/HeJ and C3H/HeN are LPS-responder and LPS-non-responder mice, respectively (38,39). As a result, the discrepancy in the response of DSS in mice might be due to differences in the substrains. In the current study, the highest incidence of colonic tumors was

found in Balb/c. C57BL/6N had the second highest incidence among the strains tested. On the other hand, C3H/HeN and DBA/2N had only a few benign colonic tumors (adenomas). The shortening of colon length in the mice that received DSS is one of the biological markers of severity of colonic inflammation (8–10,32,35). When comparing the colon length in mice treated with AOM and DSS with that in untreated mice, the order of the shortening rate of the colon length of mice was Balb/c (7%) > C57BL/6N (4%) > DBA/2N (3%) > C3H/HeN (−6%). These results suggest that the different susceptibilities of the inbred mouse strains to AOM/DSS-induced colon carcinogenesis might correlate with different sensitivities to AOM or DSS, with only slight contradictions among the substrains.

AOM is widely used as a colonic carcinogen to investigate the pathogenesis and modification of colon carcinogenesis in rodents (11–13). AOM requires metabolic activation to exert its carcinogenic action. Cytochrome P450 (CYP) is known to play a prominent role in the modulation of the xenobiotic metabolism, including chemical carcinogens. CYP 2E1 is one of the important factors for converting AOM to methylazoxymethanol, which can produce DNA adduct formation and also produce the initiation event (40,41). Although we did not investigate the activity of CYP 2E1, it may be possible that the expression and/or content of CYP 2E1 differ among the strains examined. This may be indicated by the findings that the relative liver weight of Balb/c, which had the highest susceptibility of AOM/DSS-induced colon carcinogenesis, was higher than that of other strains of mice in the current study (data not shown).

The influence of nitrosation stress caused by DSS is also an important factor for AOM/DSS-induced mouse colon carcinogenesis, since a powerful tumor-promoting activity of DSS has been observed in this model (8,32,35,42). We found a close association between the score of nitrotyrosine and the occurrence of tumors in the current study. Nitrotyrosine-immunohistochemical scores of each strain of mice in the 'AOM → DSS' and 'DSS alone' groups were much greater than those of the 'AOM alone' and 'untreated' groups. The scores of the 'AOM → DSS' group were relatively higher than those of the 'DSS alone' group in all strains of mice and the order was Balb/c > C57BL/6N > C3H/HeN > DBA/2N in these two groups. Such inflammation could influence tumorigenesis, although the inflammation score did not completely correspond with the frequency of colonic tumors in the current study. Indeed, the score of inflammation in the mice receiving both AOM and DSS was higher than that of the mice administered DSS alone. An investigation of additional factors is needed to precisely elucidate the strain differences in the susceptibility to colon carcinogenesis. Recently Greten *et al.* (43) reported interesting findings, namely that a specific inactivation of the IκB kinase (IKK)/NF-κB pathway can attenuate the formation of inflammation-associated colon tumors in *villin-Cre/Ikkβ*$^{F/\Delta}$ mice. They also suggested that IKKβ might be involved in inflammation-related carcinogenesis.

In conclusion, we herein demonstrated the differences in the genetic susceptibility to AOM/DSS-induced colon tumorigenesis among four inbred strains (Balb/c, C3H/HeN, C57BL/6N and DBA/2N) of mice and found the Balb/c mice to be the most sensitive. Our findings suggest that the genetic background thus plays an important role in the cancer risk in colitis-related colon tumorigenesis. In addition, strain differences in the susceptibility of colon carcinogenesis induced by AOM and DSS might be influenced by the response to nitrosation stress due to inflammation as determined by the genetic background.

Acknowledgements

This work was supported in part by a Grant-in-Aid for Cancer Research, for the Third-Term Comprehensive 10-Year Strategy for Cancer Control from the Ministry of Health, Labour and Welfare of Japan; the Grants-in-Aid (No. 15-2052) for Scientific Research from the Ministry of Education, Culture, Sports, Science and Technology of Japan; and a grant (H2004-6) for Project Research from the High-Technology Center of Kanazawa Medical University.

Conflict of Interest Statement: None declared.

References

1. Jemal,A., Tiwari,R.C., Murray,T., Ghafoor,A., Samuels,A., Ward,E., Feuer,E.J. and Thun,M.J. (2004) Cancer statistics, 2004. *CA. Cancer J. Clin.*, **54**, 8–29.
2. Itzkowitz,S.H. and Yio,X. (2004) Inflammation and cancer IV. Colorectal cancer in inflammatory bowel disease: the role of inflammation. *Am. J. Physiol. Gastrointest. Liver Physiol.*, **287**, G7–G17.
3. Brostrom,O., Lofberg,R., Nordenvall,B., Ost,A. and Hellers,G. (1987) The risk of colorectal cancer in ulcerative colitis. An epidemiologic study. *Scand. J. Gastroenterol.*, **22**, 1193–1199.
4. Ekbom,A., Helmick,C., Zack,M. and Adami,H.O. (1990) Ulcerative colitis and colorectal cancer. A population-based study. *N. Engl. J. Med.*, **323**, 1228–1233.
5. Greenstein,A.J. (2000) Cancer in inflammatory bowel disease. *Mt Sinai J. Med.*, **67**, 227–240.
6. Ambs,S., Merriam,W.G., Bennett,W.P., Felley-Bosco,E., Ogunfusika,M.O., Oser,S.M., Klein,S., Shields,P.G., Billiar,T.R. and Harris,C.C. (1998) Frequent nitric oxide synthase-2 expression in human colon adenomas: implication for tumor angiogenesis and colon cancer progression. *Cancer Res.*, **58**, 334–341.
7. Macarthur,M., Hold,G.L. and El-Omar,E.M. (2004) Inflammation and Cancer II. Role of chronic inflammation and *cytokine* gene polymorphisms in the pathogenesis of gastrointestinal malignancy. *Am. J. Physiol. Gastrointest. Liver Physiol.*, **286**, G515–G520.
8. Tanaka,T., Kohno,H., Suzuki,R., Yamada,Y., Sugie,S. and Mori,H. (2003) A novel inflammation-related mouse colon carcinogenesis model induced by azoxymethane and dextran sodium sulfate. *Cancer Sci.*, **94**, 965–973.
9. Tanaka,T., Suzuki,R., Kohno,H., Sugie,S., Takahashi,M. and Wakabayashi,K. (2005) Colonic adenocarcinomas rapidly induced by the combined treatment with 2-amino-1-methyl-6-phenylimidazo [4,5-*b*]pyridine and dextran sodium sulfate in male ICR mice possess b-catenin gene mutations and increases immunoreactivity for b-catenin, cyclooxygenase-2, and inducible nitric oxide synthase. *Carcinogenesis*, **26**, 229–238.
10. Kohno,H., Suzuki,R., Sugie,S. and Tanaka,T. (2005) b-Catenin mutations in a mouse model of inflammation-related colon carcinogenesis induced by 1,2-dimethylhydrazine and dextran sodium sulfate. *Cancer Sci.*, **96**, 69–76.
11. Hata,K., Yamada,Y., Kuno,T., Hirose,Y., Hara,A., Qiang,S.H. and Mori,H. (2004) Tumor formation is correlated with expression of b-catenin-accumulated crypts in azoxymethane-induced colon carcinogenesis in mice. *Cancer Sci.*, **95**, 316–320.
12. Yang,K., Lamprecht,S.A., Liu,Y., Shinozaki,H., Fan,K., Leung,D., Newmark,H., Steele,V.E., Kelloff,G.J. and Lipkin,M. (2000) Chemoprevention studies of the flavonoids quercetin and rutin in normal and azoxymethane-treated mouse colon. *Carcinogenesis*, **21**, 1655–1660.
13. Takahashi,M., Nakatsugi,S., Sugimura,T. and Wakabayashi,K. (2000) Frequent mutations of the b-*catenin* gene in mouse colon tumors induced by azoxymethane. *Carcinogenesis*, **21**, 1117–1120.
14. Okayasu,I., Hatakeyama,S., Yamada,M., Ohkusa,T., Inagaki,Y. and Nakaya,R. (1990) A novel method in the induction of reliable experimental acute and chronic ulcerative colitis in mice. *Gastroenterology*, **98**, 694–702.
15. Kitajima,S., Morimoto,M. and Sagara,E. (2002) A model for dextran sodium sulfate (DSS)-induced mouse colitis: bacterial degradation of DSS

does not occur after incubation with mouse cecal contents. *Exp. Anim.*, **51**, 203–206.
16. Hirono,I., Kuhara,K., Hosaka,S., Tomizawa,S. and Golberg,L. (1981) Induction of intestinal tumors in rats by dextran sulfate sodium. *J. Natl Cancer Inst.*, **66**, 579–583.
17. Tham,D.M., Whitin,J.C. and Cohen,H.J. (2002) Increased expression of extracellular glutathione peroxidase in mice with dextran sodium sulfate-induced experimental colitis. *Pediatr. Res.*, **51**, 641–646.
18. Cooper,H.S., Murthy,S., Kido,K., Yoshitake,H. and Flanigan,A. (2000) Dysplasia and cancer in the dextran sulfate sodium mouse colitis model. Relevance to colitis-associated neoplasia in the human: a study of histopathology, b-catenin and p53 expression and the role of inflammation. *Carcinogenesis*, **21**, 757–768.
19. Deschner,E.E., Hakissian,M. and Long,F.C. (1989) Genetic factors controlling inheritance of susceptibility to 1,2-dimethylhydrazine. *J. Cancer Res. Clin. Oncol.*, **115**, 335–339.
20. Festing,M.F. (1995) Use of a multistrain assay could improve the NTP carcinogenesis bioassay. *Environ. Health Perspect.*, **103**, 44–52.
21. Fujita,H., Nagano,K., Ochiai,M., Ushijima,T., Sugimura,T., Nagao,M. and Matsushima,T. (1999) Difference in target organs in carcinogenesis with a heterocyclic amine, 2-amino-3,4-dimethylimidazo [4,5-*f*]quinoline, in different strains of mice. *Jpn. J. Cancer Res.*, **90**, 1203–1206.
22. Gressani,K.M., Leone-Kabler,S., O'Sullivan,M.G., Case,L.D., Malkinson,A.M. and Miller,M.S. (1999) Strain-dependent lung tumor formation in mice transplacentally exposed to 3-methylcholanthrene and post-natally exposed to butylated hydroxytoluene. *Carcinogenesis*, **20**, 2159–2165.
23. Papanikolaou,A., Wang,Q.-S., Papanikolaou,D., Whiteley,H.E. and Rosenberg,D. (2000) Sequential and morphological analyses of aberrant crypt foci formation in mice of differing susceptibility to azoxymethane-induced colon carcinogenesis. *Carcinogenesis*, **21**, 1567–1572.
24. Tsuda,H., Naito,A., Kim,C., Fukamachi,K., Nomoto,H. and Moore,M.A. (2003) Carcinogenesis and its modification by environmental endocrine disruptors: in vivo experimental and epidemiological findings. *Jpn. J. Clin. Oncol.*, **33**, 259–270.
25. Wang,Q.S., Walsh,A., Goldsby,J.S., Papanikolaou,A., Bolt,A.B. and Rosenberg,D.W. (1999) Preliminary analysis of azoxymethane-induced colon tumorigenesis in mouse aggregation chimeras. *Carcinogenesis*, **20**, 691–697.
26. Nambiar,P.R., Girnun,G., Lillo,N.A., Guda,K., Whiteley,H.E. and Rosenberg,D.W. (2003) Preliminary analysis of azoxymethane induced colon tumors in inbred mice commonly used as transgenic/knockout progenitors. *Int. J. Oncol.*, **22**, 145–150.
27. Mahler,M., Bristol,I.J., Leiter,E.H., Workman,A.E., Birkenmeier,E.H., Elson,C.O. and Sundberg,J.P. (1998) Differential susceptibility of inbred mouse strains to dextran sulfate sodium-induced colitis. *Am. J. Physiol.*, **274**, G544–G551.
28. Stevceva,L., Pavli,P., Buffinton,G., Wozniak,A. and Doe,W.F. (1999) Dextran sodium sulphate-induced colitis activity varies with mouse strain but develops in lipopolysaccharide-unresponsive mice. *J. Gastroenterol. Hepatol.*, **14**, 54–60.
29. Pereira,M.A., Tao,L.H., Wang,W., Gunning,W.T. and Lubet,R. (2005) Chemoprevention: mouse colon and lung tumor bioassay and modulation of DNA methylation as a biomarker. *Exp. Lung Res.*, **31**, 145–163.
30. Singer,I.I., Kawka,D.W., Scott,S., Weidner,J.R., Mumford,R.A., Riehl,T.E. and Stenson,W.F. (1996) Expression of inducible nitric oxide synthase and nitrotyrosine in colonic epithelium in inflammatory bowel disease. *Gastroenterology*, **111**, 871–885.
31. Murata,M. and Kawanishi,S. (2004) Oxidative DNA damage induced by nitrotyrosine, a biomarker of inflammation. *Biochem. Biophys. Res. Commun.*, **316**, 123–128.
32. Suzuki,R., Kohno,H., Sugie,S. and Tanaka,T. (2005) Dose-dependent promoting effect of dextran sodium sulfate on mouse colon carcinogenesis initiated with azoxymethane. *Histol. Histopathol.*, **20**, 483–492.
33. Cooper,H.S., Murthy,S.N., Shah,R.S. and Sedergran,D.J. (1993) Clinicopathologic study of dextran sulfate sodium experimental murine colitis. *Lab. Invest.*, **69**, 238–249.
34. Krutovskikh, V.A. and Turusov, V.S. (1994) Tumours of the intestines. In Turusov,V.S. and Mohr,V. (eds) *Pathology of Tumors in Laboratory Animals*. Vol. 2-Tumours of the Mouse. IARC Scientific Publications No. 111. Lyon, pp. 195–221.
35. Suzuki,R., Kohno,H., Sugie,S. and Tanaka,T. (2004) Sequential observations on the occurrence of preneoplastic and neoplastic lesions in mouse colon treated with azoxymethane and dextran sodium sulfate. *Cancer Sci.*, **95**, 721–727.
36. Zingarelli,B., Szabo,C. and Salzman,A.L. (1999) Reduced oxidative and nitrosative damage in murine experimental colitis in the absence of inducible nitric oxide synthase. *Gut.*, **45**, 199–209.
37. Muller,I., Freudenberg,M., Kropf,P., Kiderlen,A.F. and Galanos,C. (1997) Leishmania major infection in C57BL/10 mice differing at the *Lps* locus: a new non-healing phenotype. *Med. Microbiol. Immunol. (Berl.)*, **186**, 75–81.
38. Watson,J., Riblet,R. and Taylor,B.A. (1977) The response of recombinant inbred strains of mice to bacterial lipopolysaccharides. *J. Immunol.*, **118**, 2088–2093.
39. Watson,J. and Riblet,R. (1974) Genetic control of responses to bacterial lipopolysaccharides in mice. I. Evidence for a single gene that influences mitogenic and immunogenic respones to lipopolysaccharides. *J. Exp. Med.*, **140**, 1147–1161.
40. Sohn,O.S., Ishizaki,H., Yang,C.S. and Fiala,E.S. (1991) Metabolism of azoxymethane, methylazoxymethanol and *N*-nitrosodimethylamine by cytochrome P450 IIE1. *Carcinogenesis*, **12**, 127–131.
41. Sohn,O.S., Fiala,E.S., Requeijo,S.P., Weisburger,J.H. and Gonzalez,F.J. (2001) Differential effects of CYP2E1 status on the metabolic activation of the colon carcinogens azoxymethane and methylazoxymethanol. *Cancer Res.*, **61**, 8435–8440.
42. Tanaka,T., Kohno,H., Suzuki,R., Hata,K., Sugie,S., Niho,N., Sakano,K., Takahashi,M. and Wakabayashi,K. (2005) Dextran sodium sulfate strongly promotes colorectal carcinogenesis in *Apc*$^{Min/+}$ mice: Inflammatory stimuli by dextran sodium sulfate results in development of multiple colonic neoplasms. *Int. J. Cancer*, in press.
43. Greten,F.R., Eckmann,L., Greten,T.F., Park,J.M., Li,Z.W., Egan,L.J., Kagnoff,M.F. and Karin,M. (2004) IKKb links inflammation and tumorigenesis in a mouse model of colitis-associated cancer. *Cell*, **118**, 285–296.

Received June 8, 2005; revised July 24, 2005; accepted July 28, 2005

Int. J. Cancer: **118,** 2232–2236 (2006)

Predominant T helper type 2-inflammatory responses promote murine colon cancers

Emi Osawa[1,2], Atsushi Nakajima[2], Toshio Fujisawa[2], Yuki I. Kawamura[1,3], Noriko Toyama-Sorimachi[1], Hitoshi Nakagama[4] and Taeko Dohi[1]*

[1]*Department of Gastroenterology, Research Institute, International Medical Center of Japan, Tokyo, Japan*
[2]*Gastroenterology Division, Yokohama City University School of Medicine, Yokohama, Japan*
[3]*GS platZ Co. Ltd., Tokyo, Japan*
[4]*Biochemistry Division, National Cancer Center Research Institute, Tokyo, Japan*

Colon cancer is one of the most serious complications of inflammatory bowel diseases, especially ulcerative colitis (UC). Previous studies have shown that characteristic immunological event during inflammation in UC is the expression of T helper-type 2 (Th2) cell-derived cytokines. In this study, we investigated the influence of a predominant Th2-type cytokine response in colitis on carcinogen-induced colon tumors. Wild type (WT), interferon gamma (IFN-γ) gene deficient (−/−) [Th2 dominant] or interleukin (IL)-4$^{-/-}$ [Th1-dominant] mice of BALB/c background were used in this study. To compare tumor formation, mice were given the carcinogen azoxymethane (AOM) and intrarectal administration of trinitrobenzene sulfonic acid (TNBS), to induce colitis. Thirty-three weeks after initial treatment, the total colon was examined. When IFN-γ$^{-/-}$ mice were treated with AOM and TNBS, significantly higher number of tumors were seen (8.4 ± 1.7) than in WT (3.3 ± 2.9) or IL-4$^{-/-}$ (3.1 ± 3.4) mice, which received identical treatments. A separate set of experiment, using less doses of AOM and TNBS also showed the higher frequency of tumor formation in IFN-γ$^{-/-}$ mice than in IL-4$^{-/-}$ mice. Histologically, the tumors were well- or moderately-differentiated adenocarcinomas. No invasion into the submucosal or serosal layers of the intestine was seen. In immunohistological staining, some tumors in IFN-γ$^{-/-}$ mice showed distinct nuclear expression of β-catenin, in contrast to the strong membrane staining seen in tumors of IL-4$^{-/-}$ mice. In conclusion, colonic inflammation associated with Th2-donimant cytokine responses enhanced the formation of malignant neoplasms.
© *2005 Wiley-Liss, Inc.*

Key words: colitis; cancer; interferon-γ; interleukin-4; carcinogenesis

Colorectal cancer is one of the most serious complications in inflammatory bowel diseases (IBD), including ulcerative colitis (UC) and Crohn's disease (CD).[1] Of note, patients with longstanding, extensive UC have a high cancer risk, ~16.5% at 30 years, after initial diagnosis.[2,3] It has long been noted that cancer arises from regions of chronic inflammation, and the inflammatory cells and cytokines of the immune system found in tumors are more likely to contribute to tumor growth and progression.[4] In animal models, colitis induced by dextran sulfate sodium (DSS) are associated with dysplasia and cancer.[5–7] Recent studies on liver cancer[8] and colon cancer[9] models suggested that transcription factor NF-κB, which is a key player of inflammatory responses, does not affect initiation, but acts in tumor promotion. Thus, inflammation may significantly affect the process of cancer in UC. In fact, cancers in UC have several distinct features from colorectal cancers in non-IBD patients.[10] First, tumors in UC are often multiple, which is to be expected from precancerous dysplastic changes found in UC mucosa. Second, cancer in UC is often flat and infiltrating. Third, there is a higher incidence of high-grade, mucinous carcinomas than seen in non-IBD cancer. At a molecular level, p53 gene mutations or p53 protein overexpression, which is a late event in the development of sporadic colorectal carcinoma, have been commonly reported as early events in the dysplasia–carcinoma sequences in UC-associated carcinomas.[11–14] These results provide evidence that UC-associated cancer may develop along a pathway that is different from that of sporadic colorectal cancer.

Although pathogenesis of IBD is unknown, fluctuating but constant inflammatory responses at the local site is the major pathological finding. Past studies have shown that local immunological events during chronic inflammation in UC and CD are different. The presence of activated Th1 cells in the intestine is the characteristic of CD, with high expression of interferon gamma (IFN-γ) and tumor necrosis factor alpha (TNF-α).[15,16] On the other hand, elevated expression of T helper-type 2 (Th2) cell-derived cytokines is often seen in UC.[17,18] By use of various murine models, we and others have shown that such distinct cytokine responses actually involved in the unique pathological changes in CD and UC. For example, we noted distinct pathological differences in the hapten-induced colitis in Th1 *versus* Th2-dominant mice.[19,20] In Th2 dominant mice, fibrosis and diffuse atrophic changes in epithelial cells were seen, while acute ulcers were the major lesions of colitis in Th1 dominant mice. Other groups have reported that administration of the sensitizing agent, oxazolone, induced colitis with diffuse epithelial damage. In this model, a Th2 type cytokine, interleukin (IL)-13 was the major effector cytokine.[21,22] Further, transfer of Th2-dominant T cells to T cell-deficient recipient mice resulted in ileal villus atrophy and goblet cell metaplasia,[23] while transfer of Th1 dominant T cells induced erosive gastritis with enhanced surface epithelial cell apoptosis.[24] These results suggest that a predominance of either Th1- or Th2-type cytokines in inflammatory responses has a major influence on the pathology and tissue remodeling in the chronic inflammation, and eventually affects controlling epithelial cell differentiation, as well as their turnover. Thus, differential upregulation of inflammatory cytokines in UC may directly contribute to malignant progression. However, data on the participation of a predominance of Th1 or Th2 cytokines in mucosal immunity in colonic carcinogenesis is limited.

The possible factors which lead to dysplasia and malignant transformation in UC need to be more thoroughly investigated. In this study, we used models of Th1- or Th2-dominant colitis model together with azoxymethane (AOM)-induced carcinogenesis and sequential and morphological analysis, paying particular attention to the tissue tropism of carcinogenesis. Our findings show that a Th2 cytokine dominant colitis increases the frequency and changes in pathological features of colonic neoplasms.

Abbreviations: AOM, azoxymethane; DSS, dextran sulfate sodium; GI, gastrointestinal; H&E, hematoxylin and eosin; IFN, interferon; IL, interleukin; TNBS, trinitrobenzene sulfonic acid; TNF, tumor necrosis factor.

Grant sponsors: Ministry of Health, Labor, and Welfare; International Health Cooperation Research; Ministry of Education, Culture, Sports, Science, and Technology; Japan Health Sciences Foundation and Organization; Organization for Pharmaceutical Safety and Research.

***Correspondence to:** Department of Gastroenterology, Research Institute, International Medical Center of Japan, 1-21-1 Toyama, Shinjuku-ku, Tokyo 162-8655, Japan. Fax: +81-3-3202-7364.
E-mail: dohi@ri.imcj.go.jp

Received 10 August 2005; Accepted 29 September 2005
DOI 10.1002/ijc.21639
Published online 5 December 2005 in Wiley InterScience (www.interscience.wiley.com).

Publication of the International Union Against Cancer